Resveratrol suppresses hepatic fatty acid synthesis and increases fatty acid β-oxidation via the microRNA-33/SIRT6 signaling pathway

CHUNQIAO LIU[1-3], XINYAN PAN[1-3], ZHIHUA HAO[4], XING WANG[2], CHAO WANG[2] and GUANGYAO SONG[1,2]

[1]Department of Internal Medicine, Hebei Medical University, Shijiazhuang, Hebei 050000, P.R. China;
[2]Hebei Key Laboratory of Metabolic Diseases, Hebei General Hospital, Shijiazhuang, Hebei 050051, P.R. China;
[3]Department of Endocrinology, Hebei General Hospital, Shijiazhuang, Hebei 050051, P.R. China;
[4]Department of Health Care, Hebei General Hospital, Shijiazhuang, Hebei 050051, P.R. China

Received September 26, 2023; Accepted February 23, 2024

DOI: 10.3892/etm.2024.12615

Abstract. Hyperlipidemia is a strong risk factor for numerous diseases. Resveratrol (Res) is a non-flavonoid polyphenol organic compound with multiple biological functions. However, the specific molecular mechanism and its role in hepatic lipid metabolism remain unclear. Therefore, the aim of the present study was to elucidate the mechanism underlying how Res improves hepatic lipid metabolism by decreasing microRNA-33 (miR-33) levels. First, blood miR-33 expression in participants with hyperlipidemia was detected by reverse transcription-quantitative PCR, and the results revealed significant upregulation of miR-33 expression in hyperlipidemia. Additionally, after transfection of HepG2 cells with miR-33 mimics or inhibitor, western blot analysis indicated downregulation and upregulation, respectively, of the mRNA and protein expression levels of sirtuin 6 (SIRT6). Luciferase reporter analysis provided further evidence for binding of miR-33 with the SIRT6 3'-untranslated region. Furthermore, the levels of peroxisome proliferator-activated receptor-γ (PPARγ), PPARγ-coactivator 1α and carnitine palmitoyl transferase 1 were increased, while the concentration levels of acetyl-CoA carboxylase, fatty acid synthase and sterol regulatory element-binding protein 1 were decreased when SIRT6 was overexpressed. Notably, Res improved the basic metabolic parameters of mice fed a high-fat diet by regulating the miR-33/SIRT6 signaling pathway. Thus, it was demonstrated that the dysregulation of miR-33 could lead to lipid metabolism disorders, while Res improved lipid metabolism by regulating the expression of miR-33 and its target gene, SIRT6. Thus, Res can be used to prevent or treat hyperlipidemia and associated diseases clinically by suppressing hepatic fatty acid synthesis and increasing fatty acid β-oxidation.

Correspondence to: Professor Guangyao Song, Hebei Key Laboratory of Metabolic Diseases, Hebei General Hospital, 348 Heping West Road, Shijiazhuang, Hebei 050051, P.R. China
E-mail sguangyao2@163.com

Abbreviations: ACC, acetyl-CoA carboxylase; ALT, alanine aminotransferase; AST, aspartate aminotransferase; AUC, area under the receiver operating characteristic curve; CG, control group; CON, control; CPT1, carnitine palmitoyl transferase 1; FASN, fatty acid synthase; FBG, fasting blood glucose; HbA1c, glycated hemoglobin A1c; HDL-C, high-density lipoprotein cholesterol; HFD, high-fat diet; ITT, insulin tolerance test; LDL-C, low-density lipoprotein cholesterol; MDA, malondialdehyde; miR-33, microRNA-33; MT, mutant-type; ND, normal diet; OGTT, oral glucose tolerance test; PA, palmitate; PPARγ, peroxisome proliferator-activated receptor-γ; PGC1α, PPARγ-coactivator 1α; QUICKI, quantitative insulin sensitivity check index; Res, resveratrol; RT-qPCR, reverse transcription-quantitative PCR; SIRT6, sirtuin 6; SREBP1, sterol regulatory element-binding protein 1; TC, total cholesterol; TG, triglycerides; WT, wild-type

Key words: hyperlipidemia, Res, microRNA, miR-33, SIRT6

Introduction

Hyperlipidemia is also referred to as lipid metabolism disorder or lipid metabolism abnormality. Hyperlipidemia is a systemic disorder of lipid metabolism caused by various factors, such as elevated triglycerides (TG), total cholesterol (TC) and/or low-density lipoprotein cholesterol (LDL-C), and the reduction of high-density lipoprotein cholesterol (HDL-C) (1). Unhealthy diet and excessive energy intake make hyperlipidemia a chronic disease with an increasing incidence worldwide (1,2). Hyperlipidemia is a strong risk factor for numerous diseases, such as diabetes, atherosclerosis and cardiovascular disease (3-5). Therefore, preventing and treating hyperlipidemia are effective and common methods to reduce the incidence of cardiovascular disease and other chronic diseases (6). Hyperlipidemia should be prevented and treated as early as possible to reduce the incidence of associated diseases (7).

MicroRNAs (miRNAs/miRs) have emerged as critically important post-transcriptional regulators of disease pathogenesis. A number of miRNAs have been identified as critical regulators of cellular lipid and lipoprotein metabolism (8), including the miR-33 family (9). The miRNAs of this family

comprise miR-33a and miR-33b, which are encoded within the introns of the sterol regulatory element-binding protein (SREBP)2 and 1 genes, respectively (10,11). Although the miR-33 isoforms differ in two nucleotides in their mature forms, they share the same seed sequence and repress the same target genes (12). The miR-33 family is one of the most well-studied miRNA families as a potential therapeutic target to treat numerous diseases, including atherosclerosis, obesity and diabetes (13-15). Specifically, the miR-33 family serves key roles in regulating cholesterol and fatty acid homeostasis, controlling HDL-C biogenesis and cholesterol efflux by regulating ATP binding cassette subfamily A member 1 (ABCA1) gene expression, and regulating cellular functions, such as macrophage activation, mitochondrial biogenesis and autophagy (16). Furthermore, in the liver, miR-33 regulates reverse cholesterol transport by targeting factors involved in HDL-C biogenesis (ABCA1) and the cholesterol reverse transport process, and bile acid secretion and synthesis (17,18). Hepatic miR-33 deficiency not only improves regulation of glucose homeostasis but also prevents the development of fibrosis and inflammation (19,20). Thus, miR-33 deficiency can attenuate non-alcoholic fatty liver disease-non-alcoholic steatohepatitis-hepatocellular carcinoma progression (21,22).

Recent research has revealed that dietary polyphenols, including curcumin (23), resveratrol (Res) (24) and epigallocatechin gallate (25), modulate miRNA expression. Among these, Res is a non-flavonoid polyphenol organic compound and has now been identified in >70 plants, including grapes, *Polygonum cuspidatum* and *Veratrum nigrum* (26,27). Multiple studies have confirmed that Res has multiple biological functions, including regulating lipid metabolism, anti-inflammatory effects, mitochondrial protection and/or autophagy induction, and anti-oxidation (28-35).

The liver is essential for energy homeostasis and serves an active role in synthesis, storage and redistribution of glucose and free fatty acids (36). Res and atorvastatin have been used to treat high-fat diet (HFD) intake-induced non-alcoholic fatty liver disease by targeting genes involved in cholesterol metabolism and miR-33 (37). Additionally, Res and epigallocatechin gallate bind directly and distinctively to miR-33a and miR-122, and modulate their levels in hepatocytes (38). Therefore, the specific molecular mechanism underlying the effects of miR-33 and its role in hepatic lipid metabolism are unclear. Hence, the aim of the present study was to elucidate how Res improves hepatic lipid metabolism by targeting miR-33.

Materials and methods

Study subjects. The present study was performed at the Physical Examination Center of Hebei General Hospital (Shijiazhuang, China) and was approved by the Hebei General Hospital Ethics Committee (2018 Scientific Research Ethics Review; approval no. 39; Shijiazhuang, China). All of the clinical samples were obtained from the Physical Examination Center of Hebei General Hospital. A total of 36 subjects with elevated blood lipids in the physical examination population between May 1, 2021 and November 30, 2021 were randomly selected as the hyperlipidemia group (27 men, 9 women; mean age, 65.50±7.71 years; age range, 50-83 years). Another 36 healthy subjects matched for age and sex with the subjects in the hyperlipidemia group were randomly selected during the same period from the Physical Examination Center of Hebei General Hospital as the normal control group (CG group; 27 men, 9 women; mean age, 69.11±8.81 years; age range, 43-83 years). All participants provided written informed consent. The diagnostic criteria for hyperlipidemia were in accordance with the Guidelines for the Prevention and Treatment of Dyslipidemia in Chinese Adults (Revised Edition 2016) (2), which are as follows: Plasma TC ≥6.2 mmol/l (240 mg/dl), TG ≥2.3 mmol/l (200 mg/dl), LDL-C ≥4.1 mmol/l (160 mg/dl) or HDL-C <1.0 mmol/l (40 mg/dl) in adults after a 12-h fast. Hyperlipidemia was diagnosed if any one criterion was met. Participants taking aspirin, angiotensin-converting enzyme inhibitors, angiotensin receptor blockers or statins within the previous 2 months were excluded from the study. Participants with chronic liver disease (including hepatitis B virus carriers), kidney disease, thyroid insufficiency or abnormalities, hypertension, diabetes, blood system disorders, mental disorders, acute and chronic infectious diseases, autoimmune diseases, tumors, pregnancy, lactation, long-term oral contraceptive use, and/or recent surgical history were excluded. The inclusion criteria for the CG group were as follows: No history of hypertension, diabetes mellitus and other chronic diseases; blood glucose 3.9-6.1 mmol/l; and the following blood lipid concentration levels: TC <5.2 mmol/l, TG <1.7 mmol/l and LDL-C <3.4 mmol/l.

Blood samples. Fasting blood samples (5 ml) were collected from each participant and placed in a BD Vacutainer SST tube (Becton, Dickinson and Company). Peripheral blood mononuclear cells (PBMCs) were isolated from fasting blood samples by Ficoll-Paque density gradient centrifugation (20˚C; 500 x g; 25 min) for miR-33 and sirtuin 6 (SIRT6) detection by reverse transcription-quantitative PCR (RT-qPCR). Biochemical tests [TC, TG, HDL-C, LDL-C, aspartate aminotransferase (AST), alanine aminotransferase (ALT) and fasting blood glucose (FBG)] were performed using an automatic biochemical detection instrument at the Clinical Laboratory of Hebei General Hospital. Glycated hemoglobin (HbA1c) was analyzed at Hebei Key Laboratory of Metabolic Diseases (Shijiazhuang, China) using an automatic glycohemoglobin analyzer (ADAMS A1c HA-8180; ARKRAY, Inc.) at 25˚C.

Animal experiments. A total of 24 C57BL/6J mice (male; age, 8 weeks; weight, 22.0±2.0 g) were purchased from Beijing Vital River Laboratory Animal Technology Co., Ltd. The mice were housed in the animal laboratory at the Hebei Key Laboratory of Metabolic Diseases (temperature, 21-23˚C; humidity, 40-60%; and 12/12-h light/dark cycle) with constant access to food and water. All experimental procedures were approved (2022 Scientific Research Ethics Review; approval no. 217) by the Animal Care and Use Committee of Hebei General Hospital (Shijiazhuang, China) and complied with the Animal (Scientific Procedures) Act 1986 and associated guidelines (39).

After 1 week of adaptive feeding, the mice were randomly divided into three groups, with 8 mice in each group. The diet for the normal diet (ND) group was an ordinary diet (D12450J formula, consisting of 20% protein, 70% carbohydrate, 10%

fat and 3.85 kcal/g). The model mice were fed a HFD (D12492 formula, consisting of 20% protein, 20% carbohydrate, 60% fat and 5.24 kcal/g). The Res mice were fed a HFD and a Res-based dietary supplement (60 mg/kg). All feed was purchased from Beijing Huafukang Biotechnology Co., Ltd. All mice were fed the respective diets for 6 weeks, after which they were euthanized by CO_2 asphyxiation (flow rate, 4 l/min; 30% vol/min) (40,41), and cervical dislocation was performed when the mice exhibited respiratory arrest and unconsciousness. Complete death was confirmed by cardiac arrest and dilated pupils. Blood samples were collected in tubes containing ethylenediaminetetraacetic acid (1.5 mg/ml) and centrifuged at 1,375 x g at 4˚C for 15 min. The plasma was collected and stored at -80˚C. Mice livers were quickly removed. Part of the liver tissues were snap-frozen in liquid nitrogen after washing with cold phosphate-buffered saline and stored at -80˚C for further analysis. Part of the liver tissues were fixed in 4% paraformaldehyde at 25˚C for 24 h for H&E staining.

Body weight and food intake measurement. The body weight and food intake of the mice in each group were measured at baseline and weekly thereafter until 6 weeks after baseline.

Detection of serum glucose and lipids in mice. Serum glucose levels were determined using a glucose assay kit (cat. no. 60408ES60; Shanghai Yeasen Biotechnology Co., Ltd.). The TG content assay kit (cat. no. D799796-0100; Sangon Biotech Co., Ltd.) was used to detect TG levels. The TC assay kit (cat. no. A111-1-1), LDL-C assay kit (cat. no. A113-2-1), HDL-C assay kit (cat. no. A112-1-1), ALT assay kit (cat. no. C009-3-1) and AST assay kit (cat. no. C010-3-1) were purchased from Nanjing Jiancheng Bioengineering Institute, and were used to detect the concentrations of TC, LDL-C, HDL-C, ALT and AST. Serum malondialdehyde (MDA) concentration levels were measured using a lipid peroxidation MDA assay kit (cat. no. S0131S; Beyotime Institute of Biotechnology). All protocols were performed in accordance with the manufacturers' instructions.

Oral glucose tolerance test (OGTT) and insulin tolerance test (ITT). After feeding for 6 weeks, glucose (1 g/kg) was given to each mouse via an orogastric tube for the OGTT. Blood glucose was measured immediately after glucose administration and 15, 30, 60 and 120 min after administration. A total of 24 h after the OGTT, the ITT was performed after a 12-h fast. The mice were injected intraperitoneally with insulin (1.5 IU/40 g; Tonghua Dongbao Pharmaceutical Co., Ltd.), and blood glucose was measured immediately after injection and 15, 30, 60 and 120 min after injection. The area under the receiver operating characteristic curve (AUC) for the OGTT was calculated using the trapezoidal method. The quantitative insulin sensitivity check index (QUICKI) was used to assess insulin sensitivity, as follows: QUICKI=1/[(log fasting blood glucose (mmol/l)+log fasting plasma insulin (μU/ml)].

Histomorphometric comparison of mouse liver tissues

H&E staining. Parts of the liver tissues were taken and fixed in 4% paraformaldehyde at 25˚C for 24 h. Subsequently, the tissues were embedded in paraffin wax, cut into 5-μm-thick sections, deparaffinized in xylene at 25˚C and rehydrated in a reverse-gradient series of ethyl alcohol (100, 95, 80 and 75%). The sections were stained with hematoxylin at 25˚C for 10 min and stained with eosin at 25˚C for 3 min, and visualized under a light microscope.

Oil Red O staining. Parts of the fresh liver tissues were taken and embedded in optimum cutting temperature compound, quickly frozen, and then sliced into 6-μm tissue sections. The sections were washed with PBS, stained with Oil red O working solution (6:4, oil red stock solution:distilled water; Oil red O: WSIG20100803; Sinopharm Chemical Reagent Co., Ltd.) at room temperature for 15 min and washed three times with PBS to remove the excess Oil red O dye. Subsequently, the sections were stained with Harris's hematoxylin (20151216; Nanjing Jiancheng Bioengineering Institute) for 3 min at 25˚C. The morphological features of the liver sections were observed under a light microscope.

Cell culture. HepG2 cells (human liver cancer cells) were purchased from Procell Life Science & Technology Co., Ltd., and cultured in complete DMEM (Gibco; Thermo Fisher Scientific, Inc.) supplemented with 10% fetal bovine serum (Sangon Biotech Co., Ltd.) and 1% penicillin/streptomycin (Sangon Biotech Co., Ltd.) at 37˚C with 5% CO_2. HepG2 cells were immersed in normal medium and medium containing 0.25 mmol/l palmitate (PA) for 24 h. At the end of the stimulation period, the cells were washed three times with PBS and fixed with 4% paraformaldehyde for 10 min at 37˚C. Subsequently, cells were washed twice with PBS, then stained with 0.5% Oil red O for 30 min at 37˚C. After staining, the cells were washed once with 60% isopropanol, washed with PBS until a colorless solution was obtained, and observed under a fluorescence inverted microscope at a magnification of x50. Short tandem repeat profiling was used for authentication of HepG2 cells. HepG2 cells cultured in normal medium and transfected with miR-33 mimics, and HepG2 cells cultured in medium containing 0.25 mmol/l PA for 24 h after transfection with miR-33 inhibitor or SIRT6-pcDNA 3.1 were used to analyze the effect of transfection on lipid metabolism-related genes and lipid deposition.

Cell transfection. miR-33 mimics, inhibitor and the corresponding controls were synthesized by Shanghai GenePharma Co., Ltd. For miR-33 mimics transfection, the HepG2 cells were seeded in 6-well plates at a density of $5x10^5$ cells/well. When 70-80% confluence was reached, cells were divided into three groups: CON (liposome), NC mimics (liposome + mimics control sequence) and miR-33 mimics (liposome + miR-33 mimics). The CON group was the control group, in which cells were transfected without any sequence. The NC mimics group was the scrambled negative control. The sequence of the corresponding controls (100 nmol/l) was 5'-GGUCUUACGUCAGUCACAAUAUCUG-3'. Cells were transfected using Lipofectamine® 3000 Transfection Reagent (cat. no. L3000015; Thermo Fisher Scientific, Inc.) according to the manufacturer's protocol. The cells were transfected for 6 h at 37˚C in a cell incubator with 5% CO_2, and then the medium was replaced with fresh DMEM. In the miR-33 mimics group, the cells were transfected with 100 nmol/l miR-33 mimics (5'-GUGCAUUGUAGUUGCAUUGCA-3')

using Lipofectamine® 3000 Transfection Reagent (cat. no. L3000015; Thermo Fisher Scientific, Inc.) according to the manufacturer's protocol. Cells were transfected for 6 h at 37˚C in a cell incubator with 5% CO_2, and then the medium was replaced with fresh DMEM. Subsequently, cells were incubated for 24 h in an incubator with 5% CO_2 at 37˚C, and the cells were collected for subsequent experiments.

To investigate the effect of miR-33 inhibitor transfection, HepG2 cells were divided into three groups: CON (liposome), NC inhibitor (liposome + inhibitor control sequence) and miR-33 inhibitor (liposome + miR-33 inhibitor). The CON group was the control group, in which cells were transfected without any sequence. The NC inhibitor group was transfected with 100 nmol/l scrambled negative controls (5'-GGUCUUACGUCAGUCACAAUAUCUG-3') using Lipofectamine® 3000 Transfection Reagent (cat. no. L3000015; Thermo Fisher Scientific, Inc.) according to the manufacturer's protocol. Cells were transfected for 6 h at 37˚C in a cell incubator with 5% CO_2, and then the medium was replaced with fresh DMEM. In the miR-33 inhibitor group, cells were transfected with 100 nmol/l inhibitor (5'-UGCAAUGCAACUACAAUGCAC-3') using Lipofectamine® 3000 Transfection Reagent (cat. no. L3000015; Thermo Fisher Scientific, Inc.) according to the manufacturer's protocol. Cells were transfected for 6 h at 37˚C in a cell incubator with 5% CO_2, and then the medium was replaced with fresh DMEM. Subsequently, cells were incubated for 48 h in an incubator with 5% CO_2 at 37˚C, and the cells were collected for subsequent experiments.

To investigate the effect of miR-33 inhibitor on intracellular lipid metabolism, cells were divided into three groups: PA + lipo (liposome), PA + NC inhibitor (liposome + inhibitor control sequence) and PA + miR-33 inhibitor (liposome + miR-33 inhibitor). miR-33 inhibitor or NC inhibitor (scramble control) transfection was performed as aforementioned. After transfection for 6 h at 37˚C, cells were incubated with PA (0.25 mmol/l) for 24 h in an incubator with 5% CO_2 at 37˚C and then collected for the subsequent experiments.

To investigate the effect of SIRT6 overexpression, HepG2 cells were divided into the pcDNA 3.1 group (transfected with 500 ng pcDNA 3.1) and the SIRT6-pcDNA 3.1 group (transfected with 500 ng SIRT6-pcDNA 3.1). Cells were transfected in an incubator with 5% CO_2 at 37˚C for 6 h with the aforementioned plasmids using Lipofectamine® 3000 Transfection Reagent (cat. no. L3000015; Thermo Fisher Scientific, Inc.) according to the manufacturer's protocol, and then the medium was replaced with fresh DMEM. Subsequently, cells were incubated for 24 h in an incubator with 5% CO_2 at 37˚C, and then collected for subsequent experiments.

To investigate the effect of SIRT6 overexpression on lipid metabolism, HepG2 cells divided into three groups: PA + lipo (liposome), PA + pcDNA 3.1 (liposome + 500 ng pcDNA 3.1) and PA + SIRT6-pcDNA 3.1 (liposome + 500 ng SIRT6-pcDNA 3.1). SIRT6-pcDNA 3.1 or pcDNA 3.1 transfection was performed as aforementioned. After transfection for 6 h at 37˚C, cells were incubated with PA (0.25 mmol/l) for 24 h in an incubator with 5% CO_2 at 37˚C and then collected for subsequent experiments. The human SIRT6-pcDNA 3.1 (cat. no. V38520) was purchased from Thermo Fisher Scientific, Inc.

RNA isolation and RT-qPCR. RNAs from PBMCs of participants with hyperlipidemia, three randomly selected mouse liver tissues or cultured HepG2 cells were isolated using a total RNA purification kit (Sangon Biotech Co., Ltd.). Complementary DNA synthesis was performed using the Goscript Reverse Transcriptase System (Promega Corporation) and All-in-One™ miRNA First-Strand cDNA Synthesis kit (GeneCopoeia, Inc.). The aforementioned operations were carried out in strict accordance with the manufacturer's instructions. qPCR was performed using an Applied Biosystems 7500 system (Thermo Fisher Scientific, Inc.) to detect mRNA levels using GoTaq® qPCR Master Mix (Promega Corporation) and miRNA levels using the All-in-One™ miRNA RT-qPCR detection kit (fluorophore, SYBR® Green I; GeneCopoeia, Inc.). The thermocycling conditions were as follows: Polymerase activation for 1 cycle at 95˚C for 2 min; followed by 40 cycles of 95˚C for 15 sec and 60˚C for 1 min. Relative fold changes in RNA expression were calculated using the $2^{-\Delta\Delta Ct}$ method (42). mRNA levels were normalized to GAPDH gene expression, and miRNA levels were normalized to U6 small nuclear RNA levels. The primer sequences used were as follows: Mouse (m-)SIRT6 forward, 5'-CCGGGACCTGATGCTCGCTGATGA-3' and reverse, 5'-AGCCGTGGATGCGCAGGTCAG-3'; m-FASN forward, 5'-CGGTCCCTGTGCGCCTTCC-3' and reverse, 5'TGGGGTTGTGGAAGTGCAGGTTAGG-3'; m-PPARγ forward, 5'-CCGAAGAACCATCCGATTGAAGC-3' and reverse, 5'-CCGCCAACAGCTTCTCCTTCTCG-3'; m-PGC1α forward, 5'-AAGCGAAGAGCATTTGTCAACAGCA-3' and reverse, 5'-GCGGTTGTGTATGGGACTTCTTTTT-3'; m-CPT1 forward, 5'-AGCGCTGGCAAATGACTTCCTGAG-3' and reverse, 5'-CCTGCAGCGGTGTGGGGGTGAC-3'; m-SREBP1 forward, 5'-CGCAAGGCCATCGACTACATCCG-3' and reverse, 5'-CGGCGTCTGAGGGTGGAGGGGTAA-3'; m-ACC forward, 5'-GCCCCCGAGCCAGAGGACAGTAT-3' and reverse, 5'-CCGGGAGGAGTTCTGGAAGGAGC-3'; human (h-)SIRT6 forward, 5'-CGGCCCACGCAGACCCACATG-3' and reverse, 5'-TGGGGAAGCCTGAGCGCACAT-3'; h-FASN forward, 5'-GCGGCTGCTGCTGGAAGTCACCTAT-3' and reverse, 5'-GCCGCTCACGCCCACCCAGA-3'; h-PPARγ forward, 5'-GGCCGAGAAGGAGAAGCTGTTGG-3' and reverse, 5'-CGCCCTCGCCTTTGCTTTGGT-3'; h-PGC1α forward, 5'-CCCAGAACCATGCAAATCACAATCA-3' and reverse, 5'-GACGTCTTTGTGGCTTTTGCTGTTG-3'; h-CPT1 forward, 5'-CCCGGCAAGCCCCTCCAGTT-3' and reverse, 5'-GGACATGCAGTTGGCCGTTTC-3'; h-SREBP1 forward, 5'-CGCCCTCACCCCTGTCCCCTCC-3' and reverse, 5'-GGGGCTGTGGGGTGGGGGTC-3'; h-ACC forward, 5'-CCCCACTATGAGGCCGAGCA-3' and reverse, 5'-AGCGGGAGAAGCCACGGTAAAGT-3'; m/h-GAPDH forward, 5'-TGAACGGGAAGCTCACTG-3' and reverse, 5'-GCTTCACCACCTTCTTGATG-3'; m/h-miR-33 forward, 5'-GTGCATTGTAGTTGCATTGC-3' and reverse, 5'-GTCGTATCCAGTGCAGGGT-3'; m/h-U6 forward, 5'-CTCGCTTCGGCAGCACA-3' and reverse, 5'-AACGCTTCACGAATTTGCGT-3'.

Western blotting. Liver tissues of three randomly selected mice or cultured HepG2 cells were lysed in radioimmunoprecipitation assay lysis buffer (Thermo Fisher Scientific, Inc.; 25 mM Tris, HCl pH 7.6, 150 mM NaCl, 1% NP-40, 1%

sodium deoxycholate and 0.1% SDS), and the total soluble protein was quantified using a BCA Protein Assay kit (Beijing Solarbio Science & Technology Co., Ltd.). Protein (20 μg/lane) from cell lysates was separated by 10% sodium dodecyl sulfate-polyacrylamide gel electrophoresis. Following transfer of the proteins onto polyvinylidene fluoride membranes, the membranes were blocked at room temperature for 60 min in 5% skim milk and probed with the primary antibodies overnight at 4˚C: Acetyl-CoA carboxylase (ACC; dilution, 1:2,000; cat. no. 3676; Cell Signaling Technology, Inc.), fatty acid synthase (FASN; dilution, 1:1,000; cat. no. ab128870; Abcam), SREBP1 (dilution, 1:2,000; cat. no. 557036; BD Biosciences), peroxisome proliferator-activated receptor-γ (PPARγ; dilution, 1:1,000; cat. no. 16,643-1-AP; Proteintech Group, Inc.), anti-PPARγ-coactivator 1 α (PGC1α; dilution 1:1,000; cat. no. 66,369-1-Ig; Proteintech Group, Inc.), carnitine palmitoyltransferase 1 (CPT1; dilution 1:1,000; cat. no. AF6558; Beyotime Institute of Biotechnology), SIRT6 (dilution, 1:1,000; cat. no. ab191385; Abcam) and anti-β-actin (dilution, 1:1,000; cat. no. 60008-1; Proteintech Group, Inc.). The membranes were incubated with the secondary antibodies for 2 h at room temperature. The secondary antibodies included the HRP-conjugated goat anti-rabbit antibody (dilution, 1:5,000; cat. no. ZDR-5306; OriGene Technologies, Inc.) and the HRP-conjugated goat anti-mouse antibody (dilution, 1:10,000, cat. no. ZDR-5307; OriGene Technologies, Inc.). Protein bands were visualized using enhanced chemiluminescent substrate (Pierce ECL Western Blotting substrate; Thermo Fisher Scientific, Inc.), and the band intensities were evaluated using Image J software (V1.8; National Institutes of Health).

Dual luciferase assay. The synthesized SIRT6 3'-untranslated region (UTR) was inserted into the pmirGLO vector (Promega Corporation). The mutation in the miR-33 seed-matching sequences was designed using the SIRT6 wild-type (WT) sequence generated by overlap extension PCR. SIRT6 WT and SIRT6 mutant-type (MT) reporter plasmids were designed and constructed by Guangzhou RiboBio Co., Ltd. 293T cells (Shanghai GeneChem Co., Ltd.) were cultured in High Glucose DMEM (Gibco; Thermo Fisher Scientific, Inc.) supplemented with 10% fetal bovine serum (Sangon Biotech Co., Ltd.) and 1% penicillin/streptomycin at 37˚C with 5% CO_2. The WT and MT sequences were co-transfected with the miR-33 mimic (5'-GUGCAUUGUAGUUGCAUUGCA-3'; 100 nM) or corresponding control (5'-GGUCUUACGUCAGUCACAAUAUCUG-3'; 100 nM) into 293T cells using Lipofectamine® 3000 (Invitrogen; Thermo Fisher Scientific, Inc.) at 37˚C for 6 h. After transfection for 24 h, the cells were lysed and subjected to a Dual-Luciferase Reporter Assay (Promega Corporation). Luciferase activity was measured and calculated as the ratio of firefly luciferase activity to *Renilla* luciferase activity. The experiment was repeated three times.

Statistical analysis. All experimental data are presented as the mean ± SD. All experiments were repeated at least three times to verify the trends. One-way ANOVA with Tukey's post hoc test was used for comparisons among multiple groups. Comparisons between groups were performed using an unpaired Student's t-test. Sex differences were compared using the Pearson χ^2 test. SPSS (version 25.0; IBM Corp.) was used for all analyses. $P<0.05$ was considered to indicate a statistically significant difference.

Results

Clinical and metabolic characteristics of the participants. Demographic, clinical and biochemical data were obtained from 36 participants with hyperlipidemia and 36 healthy control participants. As shown in Table I, BMI, weight, TC, TG, LDL-C, FBG, HbA1c, ALT and AST concentration levels were significantly higher, while HDL-C levels were significantly lower, in participants with hyperlipidemia compared with CG participants. No significant differences in sex, age or height were observed between the groups.

miR-33 and SIRT6 expression levels differ between participants with hyperlipidemia and CG participants. PBMCs from the hyperlipidemia group and CG were tested for miR-33 and SIRT6 expression levels and it was identified that miR-33 expression levels were significantly higher (Fig. 1A), and SIRT6 expression was significantly lower in the hyperlipidemia group compared with the CG (Fig. 1B).

Res reverses the changes in lipid metabolism and expression of miR-33 and SIRT6 in the HFD mouse model. Before investigating the underlying mechanism of Res in lipid metabolism, the mice in the HFD group were used to investigate lipid metabolism and miRNA expression in blood or liver tissues, respectively. After 6 weeks, body weights were significantly higher in the HFD group compared with the ND group. From 5 weeks, body weights were decreased significantly in the HFD + Res group compared with the HFD group (Fig. 2A). There was no significant difference in the daily food intake among the three groups (Fig. 2B). TC, TG, LDL-C, MDA, ALT and AST concentration levels were significantly higher in mice in the HFD group compared with mice in the ND group, and these levels were decreased significantly in the HFD + Res group compared with the HFD group (Fig. 2C and D). By contrast, HDL-C concentration levels were significantly lower in the HFD group compared with the ND group, and significantly increased in the HFD + Res group compared with the HFD group (Fig. 2C). Blood glucose levels were also recorded, and OGTT and ITT results are shown in Fig. 2E and G. In the OGTT, there was a significant decrease in the AUC in the HFD + Res group compared with the HFD group (Fig. 2F). Consistently, there was a statistically significant difference in QUICKI values between the HFD + Res and HFD groups (Fig. 2H).

To investigate the effect of Res on hepatic lipid deposition in mice, H&E staining and oil red O staining were performed using mouse liver tissues. H&E staining of mouse liver tissues revealed uniform cell cytoplasm in ND mice and fewer lipid droplets (Fig. 3A). In comparison, hepatocyte staining in the HFD group revealed disordered cellular structure and more lipid droplets (Fig. 3B). In the HFD + Res group, the morphology of the liver tissue and the number of lipid droplets were intermediate to those of the ND and HFD groups (Fig. 3C). Liver cell staining with oil red O showed that cells from the ND group contained blue nuclei with a small number of orange-red lipid droplets (Fig. 3D). The HFD group exhibited numerous

Table I. Comparison of the clinical characteristics and metabolic parameters between the hyperlipidemia group and CG.

Characteristics	Hyperlipidemia group (n=36)	CG (n=36)	P-value
Sex, n			1.000
Male	27	27	
Female	9	9	
Age, years	65.50±7.71	69.11±8.81	0.068
BMI, kg/m^2	24.53±2.34[a]	23.26±2.53	0.030
Weight, kg	72.11±9.80[a]	67.18±10.19	0.040
Height, cm	171.39±7.41	169.65±6.98	0.310
TC, mmol/l	6.43±0.76[a]	4.72±0.76	<0.001
TG, mmol/l	2.53±2.97[a]	0.90±0.30	0.002
LDL-C, mmol/l	4.04±0.54[a]	2.79±0.54	<0.001
HDL-C, mmol/l	1.29±0.31[a]	1.52±0.23	0.001
FBG, mmol/l	5.55±0.46[a]	5.19±0.47	0.002
HbA1c, %	6.05±0.74[a]	5.64±0.26	0.002
ALT, U/l	20.978±8.67[a]	17.08±4.71	0.020
AST, U/l	26.19±7.73[a]	22.92±5.19	0.039

[a]P<0.05 vs. CG. Sex differences were compared using the Pearson χ^2 test. An unpaired Student's t-test was used to compare data between two groups. ALT, alanine aminotransferase; AST, aspartate aminotransferase; CG, control group; FBG, fasting blood glucose; HbA1c, glycated hemoglobin A1c; HDL-C, high-density lipoprotein cholesterol; LDL-C low-density lipoprotein cholesterol; TC, total cholesterol; TG, triglycerides.

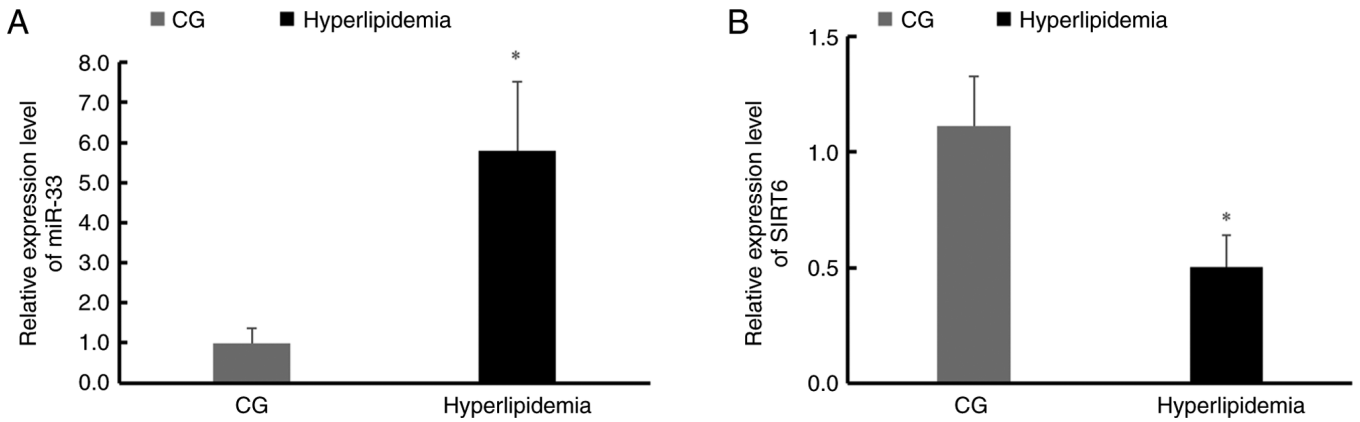

Figure 1. Relative expression levels of miR-33 and SIRT6 in peripheral blood mononuclear cells from the hyperlipidemia group and the CG. (A) Reverse transcription-quantitative PCR analysis of miR-33. (B) Reverse transcription-quantitative PCR analysis of SIRT6. Data are presented as the mean ± SD (n=36 in each group). *P<0.05 vs. CG (unpaired t-test). CG, control group; miR, microRNA; SIRT6, sirtuin 6.

orange-red lipid droplets (Fig. 3E), whereas after Res treatment, the number of lipid droplets decreased (Fig. 3F).

To gain further insights, the effect of Res on lipid metabolism and gene expression was investigated. The results revealed that miR-33 expression was significantly higher (Fig. 4A) and SIRT6 mRNA expression was significantly lower (Fig. 4B) in liver tissue of the HFD group compared with the ND group. Western blot analysis to assess SIRT6 expression in tissues revealed a significant decrease in the HFD group (Fig. 4C and D). In the HFD + Res group, Res reversed the increase in miR-33 expression and the decrease in SIRT6 expression. It was also found that mRNA expression levels (Fig. 4E) and protein expression levels (Fig. 4F and G) of ACC, FASN and SREBP1 were increased in the HFD group compared with the ND group, whereas PPARγ, PGC1α and CPT1 mRNA and protein expression levels were decreased. However, these changes in the expression levels of liver genes and proteins were reversed in the HFD + Res group (Fig. 4E-G). These findings indicated that Res improved basic metabolic parameters and changed the expression levels of metabolism-related genes in mice fed a HFD supplemented with Res.

Res reverses the changes in lipid metabolism and expression of miR-33 and SIRT6 in PA-induced HepG2 cells. To further examine the underlying mechanism, PA-induced HepG2 cells were used to investigate the effect of Res on lipid metabolism and expression levels of miR-33 and SIRT6 *in vitro*. First, a high-fat model was constructed by inducing HepG2 cells with

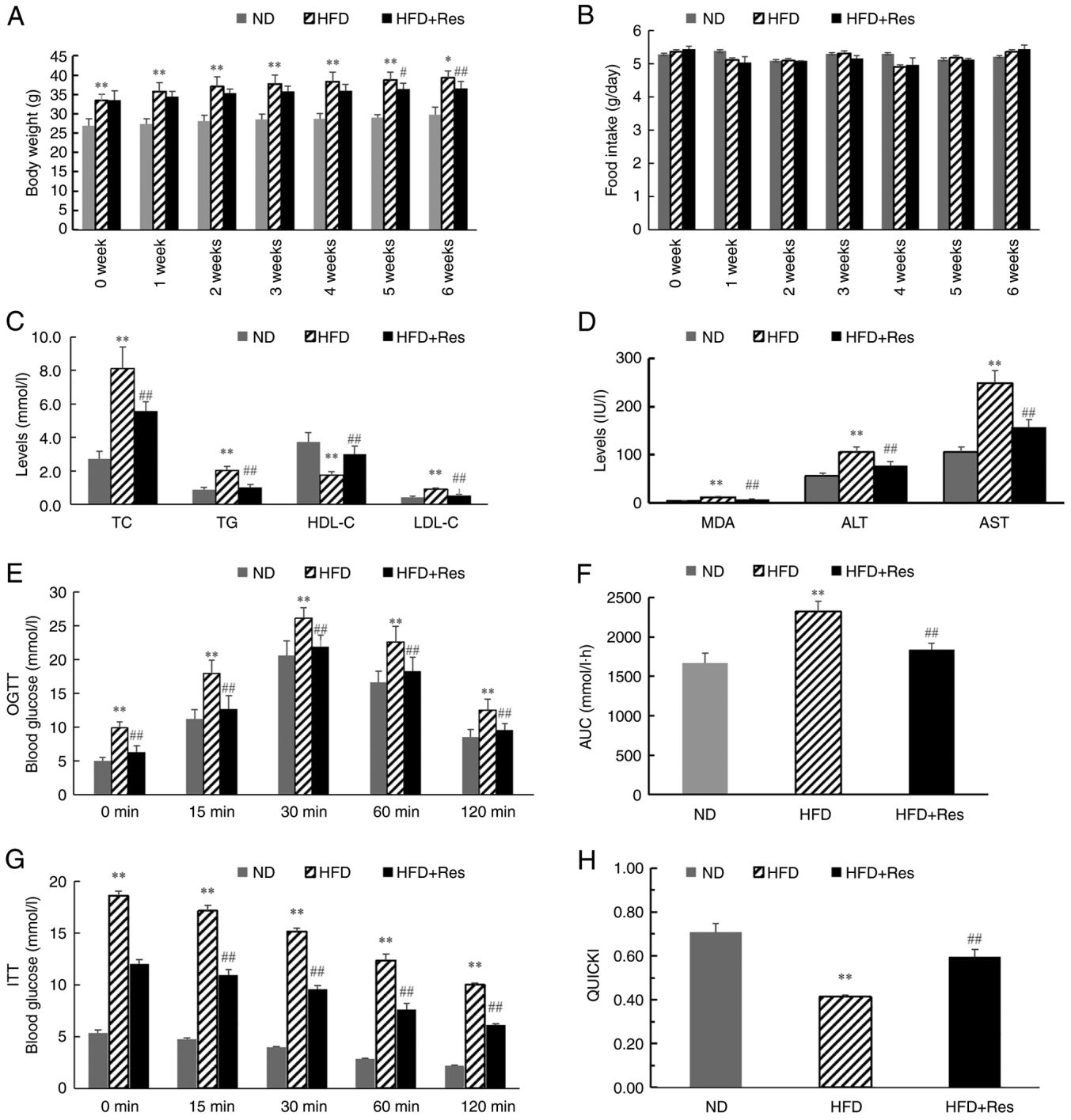

Figure 2. Effect of Res on lipid metabolism. (A) Body weights of the mice in the three groups (ND mice, and mice that received a HFD or a HFD + Res diet for 6 weeks). (B) Average daily food intake in the three groups. (C) Levels of TC, TG, HDL-C and LDL-C in the three groups after Res treatment for 6 weeks. (D) Levels of MDA, ALT and AST in the three groups after Res treatment for 6 weeks. (E) Results of OGTT. (F) AUC for OGTT. (G) Results of ITT and (H) QUICKI calculations. Data are presented as the mean ± SD (n=8 per group). *P<0.05 and **P<0.001 vs. ND group; $^{\#}$P<0.05 and $^{\#\#}$P<0.001 vs. HFD group (one-way ANOVA with Tukey's multiple comparison test). ALT, alanine aminotransferase; AST, aspartate aminotransferase; AUC, area under the receiver operating characteristic curve; HDL-C, high-density lipoprotein; HFD, high-fat diet; HFD + Res, high-fat diet supplemented with Res; ITT, insulin tolerance test; LDL-C, low-density lipoprotein cholesterol; MDA, malondialdehyde; ND, normal diet; OGTT, oral glucose tolerance test; QUICKI, quantitative insulin sensitivity check index; Res, resveratrol; TG, triglycerides; TC, total cholesterol.

PA, and changes after Res treatment were observed. It was found that lipid deposition in HepG2 cells improved after the addition of Res (Fig. 5A). Next, changes in miR-33 and SIRT6 mRNA expression were detected in PA-induced HepG2 cells. RT-qPCR analysis demonstrated that miR-33 expression was increased significantly (Fig. 5B) and mRNA levels of SIRT6 decreased significantly (Fig. 5C) in PA-induced HepG2 cells compared with CON cells. Additionally, treatment with Res decreased miR-33 expression and increased SIRT6 expression in PA-induced HepG2 cells (Fig. 5B and C). Furthermore, western blotting indicated that, with Res supplementation, protein expression levels of SIRT6, PPARγ, PGC1α and

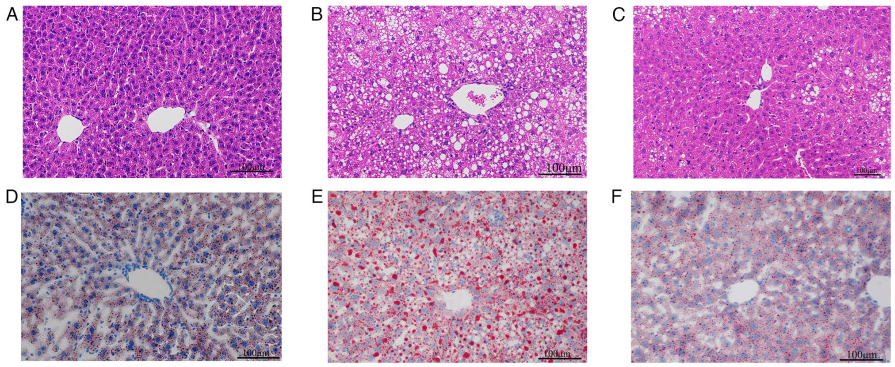

Figure 3. Histomorphological findings of hepatic lipid deposition. (A-C) H&E staining of liver tissues. (A) ND group; (B) HFD group; (C) HFD + Res group. (D-F) Oil Red O staining of liver tissues. (D) ND group; (E) HFD group; (F) HFD + Res group. Scale bar, 100 μm. HFD, high-fat diet; ND, normal diet; Res, resveratrol.

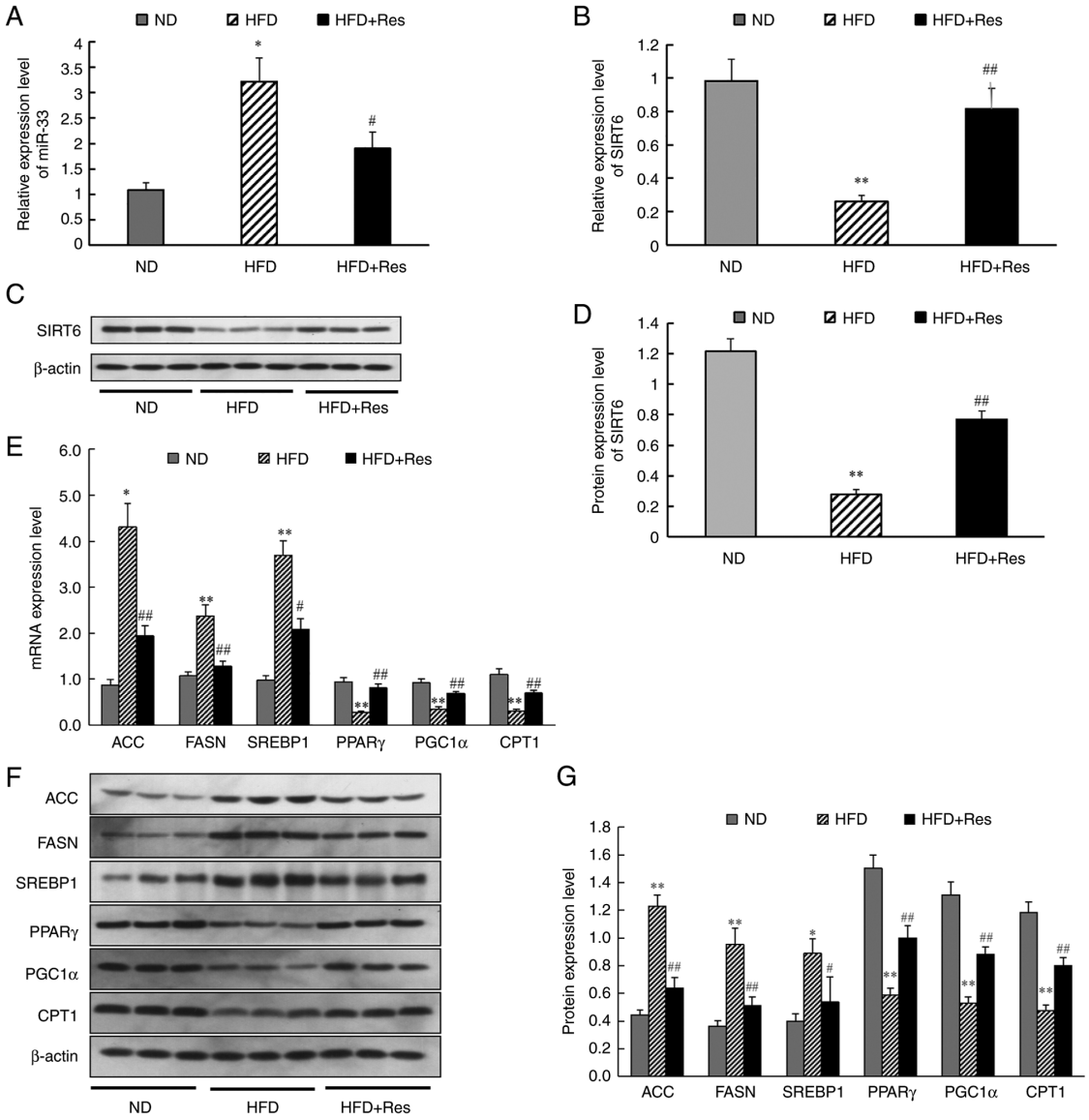

Figure 4. Effect of Res on the expression levels of miR-33, SIRT6 and genes involved in fatty acid synthesis and fatty acid β-oxidation *in vivo*. (A) Relative expression levels of miR-33 in liver tissues. (B) Relative expression levels of SIRT6 in liver tissue. (C) Protein levels of SIRT6. (D) Western blot analysis of SIRT6. (E) mRNA expression levels of genes involved in fatty acid synthesis and fatty acid β-oxidation in liver tissues. (F) Western blot analysis of ACC, FASN, SREBP1, PPARγ, PGC1α and CPT1. (G) Expression levels of proteins involved in fatty acid synthesis and fatty acid β-oxidation in liver tissues. β-actin was used as a control for the normalization of samples for western blotting. Data are presented as the mean ± SD (n=3). *P<0.05 and **P<0.001 vs. ND group; $^{\#}$P<0.05 and $^{\#\#}$P<0.001 vs. HFD group (one-way ANOVA with Tukey's multiple comparison test). ACC, acetyl-CoA carboxylase; CPT1, carnitine palmitoyl transferase 1; FASN, fatty acid synthase; HFD, high-fat diet; HFD + Res, HFD supplemented with Res; miR, microRNA; ND, normal diet; PGC1α, PPARγ-coactivator 1α; PPARγ, peroxisome proliferator-activated receptor-γ; Res, resveratrol; SIRT6, sirtuin 6; SREBP1, sterol regulatory element-binding protein 1.

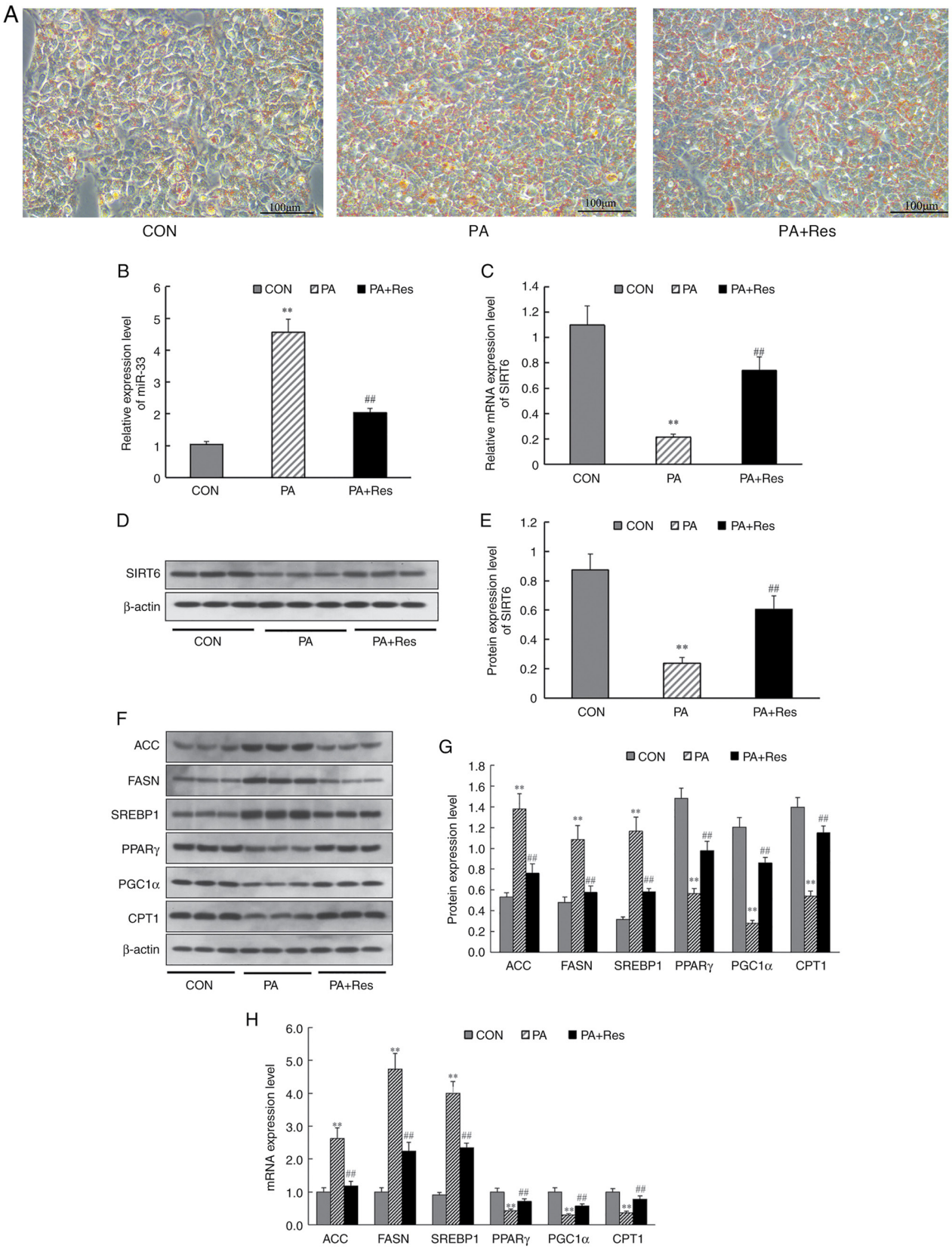

Figure 5. Effect of Res on the expression levels of miR-33, SIRT6 and genes involved in fatty acid synthesis and fatty acid β-oxidation *in vitro*. (A) Oil Red O staining of HepG2 cells. Pale blue cytosol and a small amount of orange lipid droplets were visible in CON cells. Numerous orange lipid droplets were visible in PA-treated cells. After Res treatment, the numbers of lipid droplets were decreased compared with those in PA-treated cells (Scale bar, 100 μm). (B) Relative expression levels of miR-33. (C) Relative expression level of SIRT6. (D) Western blot analysis of SIRT6. (E) Protein levels of SIRT6. (F) Western blot analysis of ACC, FASN, SREBP1, PPARγ, PGC1α and CPT1. (G) Expression levels of proteins involved in fatty acid synthesis and fatty acid β-oxidation. (H) Genes involved in fatty acid synthesis and fatty acid β-oxidation. β-actin was used as a control for the normalization of samples for western blotting. Data are presented as the mean ± SD (n=3). **P<0.001 vs. CON group; $^{\#\#}$P<0.001 vs. the PA group (one-way ANOVA with Tukey's multiple comparison test). ACC, acetyl-CoA carboxylase; CON, control; CPT1, carnitine palmitoyl transferase 1; FASN, fatty acid synthase; miR, microRNA; PA, palmitate; PGC1α, PPARγ-coactivator 1α; PPARγ, peroxisome proliferator-activated receptor-γ; Res, resveratrol; SIRT6, sirtuin 6; SREBP1, sterol regulatory element-binding protein 1.

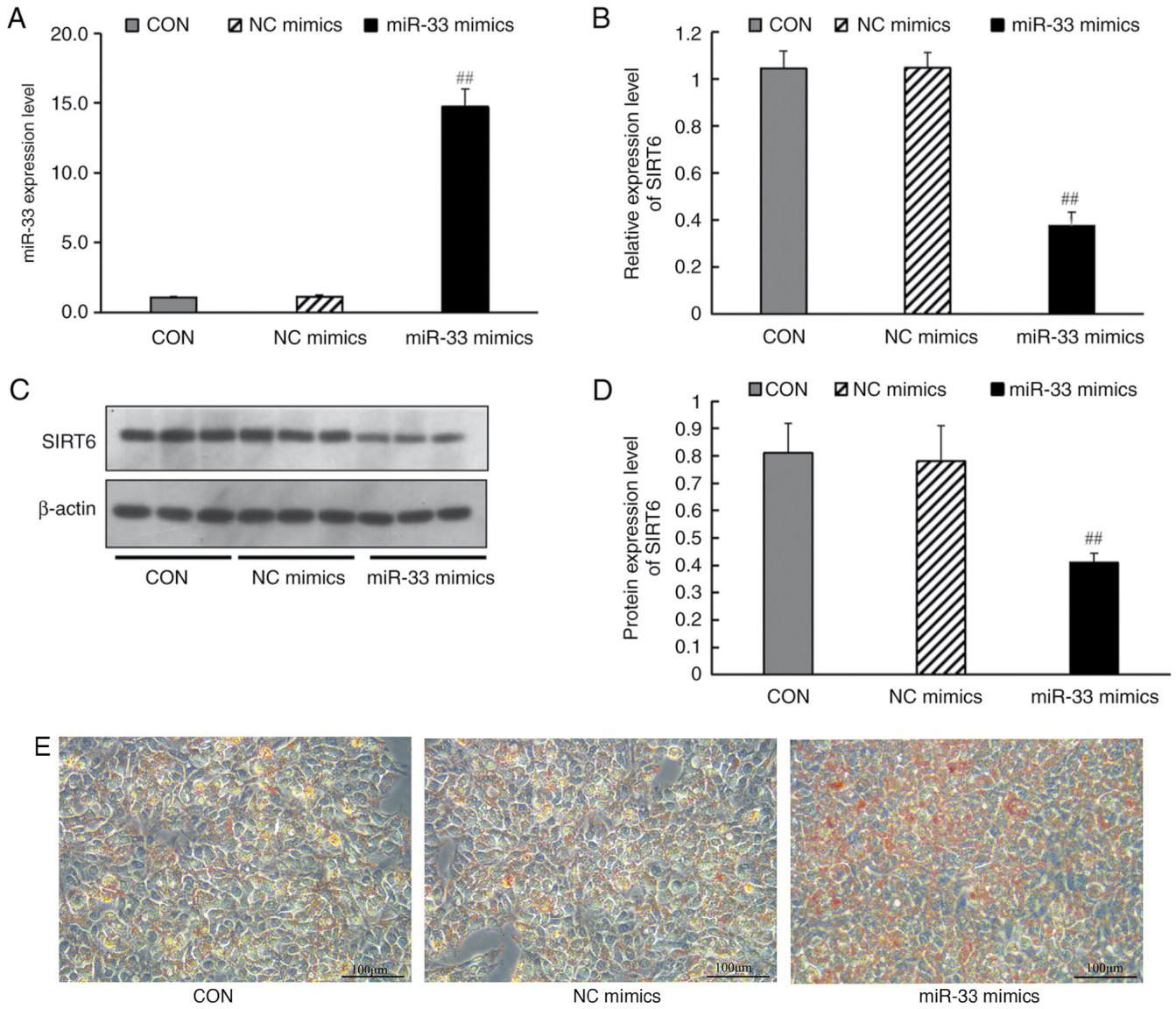

Figure 6. Effects of miR-33 mimics transfection on the expression levels of SIRT6 and lipid deposition. HepG2 cells were transfected with NC mimics or miR-33 mimics for 24 h before harvesting. (A) Expression levels of miR-33 after transfection with NC mimics or miR-33 mimics. (B) mRNA levels of SIRT6. (C) Western blot analysis of SIRT6. (D) Protein levels of SIRT6. (E) Lipid deposition in HepG2 cells after miR-33 mimics transfection. β-actin was used as a control for the normalization of samples for western blotting. Scale bar, 100 μm. Data are presented as the mean ± SD (n=3). $^{\#\#}$P<0.001 vs. NC mimics group (one-way ANOVA with Tukey's multiple comparison test). CON, liposome; NC mimics, liposome + mimics control sequence; miR-33 mimics, liposome + miR-33 mimics; miR, microRNA; SIRT6, sirtuin 6.

CPT1 (Fig. 5F and G) were increased compared with those in PA-induced HepG2 cells, whereas the expression levels of ACC, FASN and SREBP1 were decreased (Fig. 5F and G). Additionally, RT-qPCR results revealed that incubation with Res reversed mRNA expression levels of the aforementioned genes in PA-induced HepG2 cells (Fig. 5H). These results indicated that Res significantly changed the expression of metabolism-related genes *in vitro*.

miR-33 mimics transfection affects the expression of SIRT6 and lipid metabolism-related genes. 100 nmol/l miR-33 mimics or mimic controls were transfected into HepG2 cells. The results demonstrated that, after transfection with miR-33 mimic, the expression levels of miR-33 in cells were significantly increased (Fig. 6A). Transfection of miR-33 mimics (but not a negative control miRNA) led to a significant decrease in SIRT6 mRNA (Fig. 6B) and protein expression levels (Fig. 6C and D), and promoted lipid deposition in HepG2 cells (Fig. 6E).

miR-33 inhibitor transfection affects the expression of SIRT6 and lipid metabolism-related genes. miR-33 inhibitor or inhibitor controls (100 nmol/l) were transfected into HepG2 cells. The results demonstrated that, after transfection with miR-33 inhibitor, the expression levels of miR-33 in cells were significantly decreased (Fig. 7A). Similarly, miR-33 inhibition significantly increased SIRT6 mRNA expression (Fig. 7B) and protein expression compared with those in the inhibitor control group (Fig. 7C and D). HepG2 cells were induced by PA for 24 h after transfection, and then RT-qPCR was used to analyze the effect of miR-33 inhibitor transfection on lipid metabolism-related genes, and Oil Red O

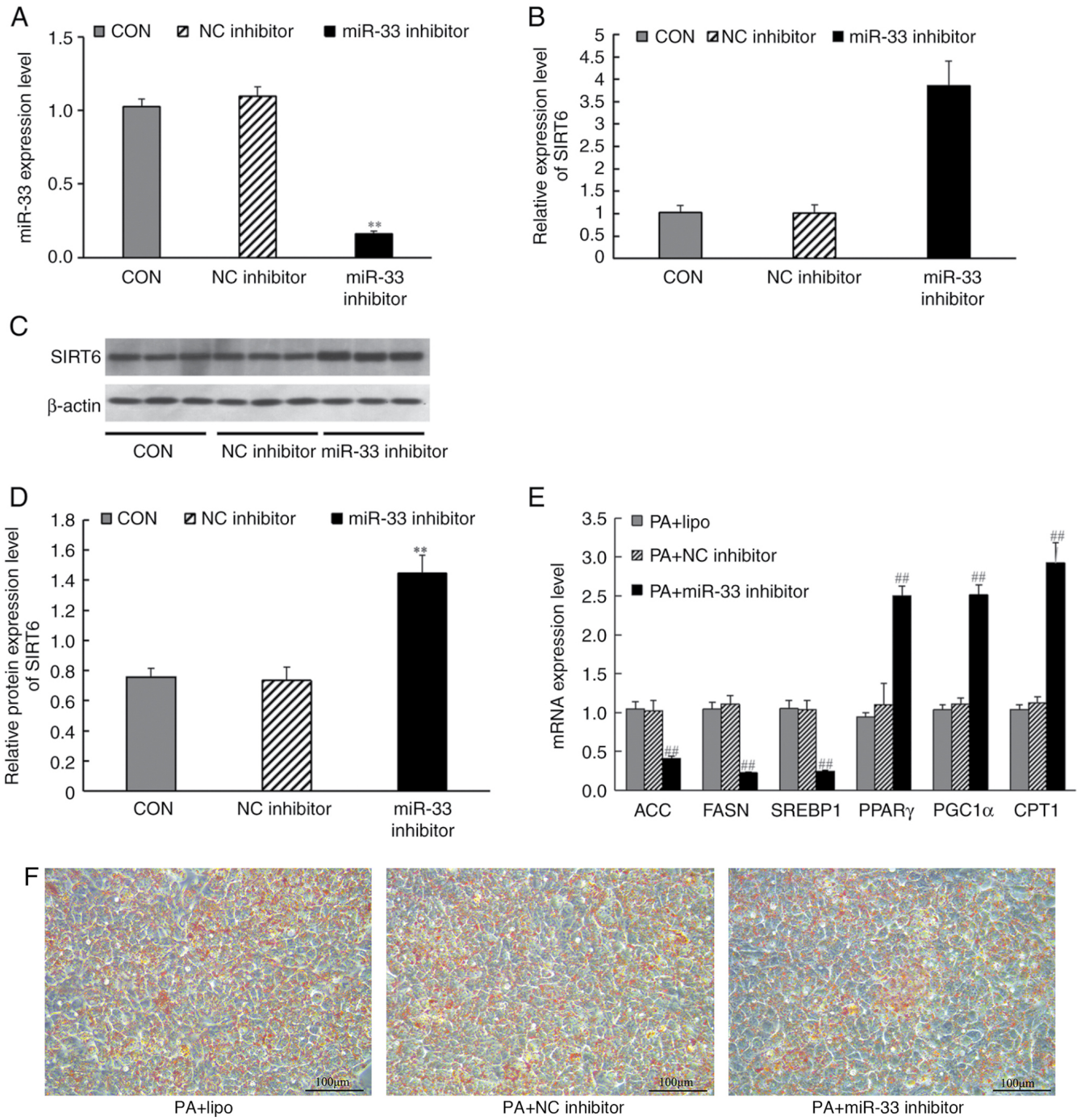

Figure 7. Effects of miR-33 inhibitor transfection on the mRNA and protein expression levels of SIRT6, and expression levels of mRNAs involved in fatty acid synthesis and fatty acid β-oxidation. HepG2 cells were transfected with miR-33 inhibitors for 24 h before harvesting. (A) Expression levels of miR-33 after transfection with miR-33 inhibitors. (B) mRNA levels of SIRT6. (C) Western blot analysis of SIRT6. (D) Protein levels of SIRT6. CON group (liposome); NC inhibitor group (liposome + inhibitor control sequence); miR-33 inhibitor group (liposome + miR-33 inhibitor). **P<0.001 vs. NC inhibitor group (one-way ANOVA with Tukey's multiple comparison test). (E) mRNA expression levels of ACC, FASN, SREBP1, PPARγ, PGC1α and CPT1, which are involved in fatty acid synthesis and fatty acid β-oxidation, in PA + HepG2 cells following miR-33 inhibitor transfection. (F) Effects of miR-33 inhibitor on intracellular lipid deposition. PA + lipo group (liposome); PA + NC inhibitor group (liposome + inhibitor control sequence); PA + miR-33 inhibitor group (liposome + miR-33 inhibitor); $^{\#\#}$P<0.001 vs. PA + NC inhibitor group (one-way ANOVA with Tukey's multiple comparison test). β-actin was used as a control for the normalization of samples for western blotting, respectively. Scale bar, 100 μm. Data are presented as the mean ± SD (n=3). ACC, acetyl-CoA carboxylase; CPT1, carnitine palmitoyl transferase 1; FASN, fatty acid synthase; miR, microRNA; PA, palmitate; PGC1α, PPARγ-coactivator 1α; PPARγ, peroxisome proliferator-activated receptor-γ; SIRT6, sirtuin 6; SREBP1, sterol regulatory element-binding protein 1.

staining was used to analyze the effect of miR-33 inhibitor on lipid deposition. RT-qPCR results revealed that transfection with the miR-33 inhibitor significantly increased the mRNA expression levels of PPARγ, PGC1α and CPT1, decreased the mRNA expression levels of ACC, FASN and SREBP1 (Fig. 7E), Simultaneously, Oil Red O staining revealed decreased lipid deposition in HepG2 cells after miR-33 inhibitor transfection (Fig. 7F).

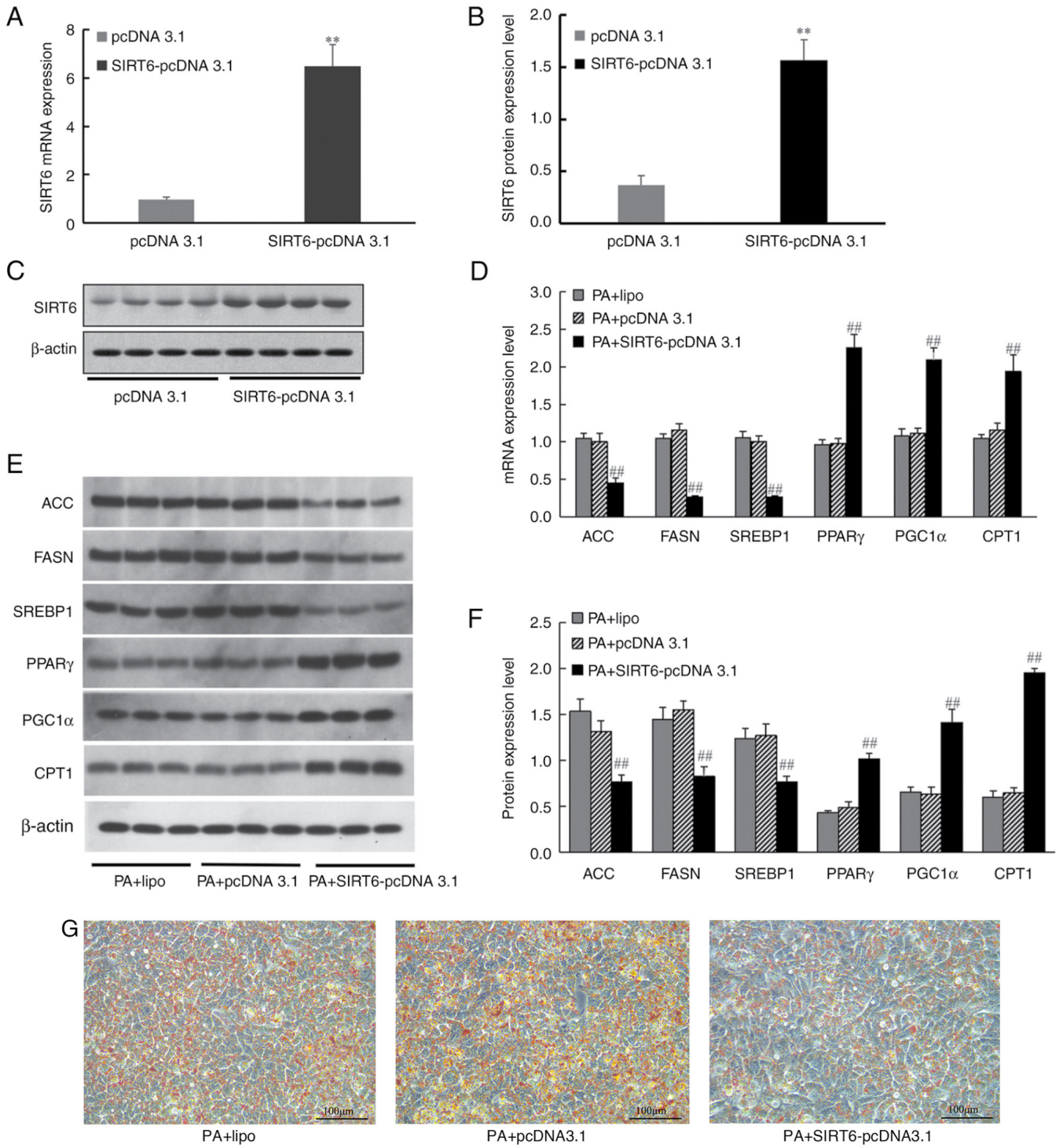

Figure 8. Effect of SIRT6 overexpression on the expression of genes involved in fatty acid synthesis and fatty acid β-oxidation. (A) mRNA expression levels of SIRT6. (B) Protein expression levels of SIRT6. (C) Western blot analysis of SIRT6. pcDNA 3.1 group (transfected with pcDNA 3.1); SIRT6-pcDNA 3.1 group (transfected with SIRT6-pcDNA 3.1) (n=3; **P<0.001 vs. pcDNA 3.1 group; unpaired t-test). (D) mRNA levels of ACC, FASN, SREBP1, PPARγ, PGC1α and CPT1 in HepG2 cells following transfection. (E) Western blot analysis of ACC, FASN, SREBP1, PPARγ, PGC1α and CPT1. (F) Protein expression levels of ACC, FASN, SREBP1, PPARγ, PGC1α and CPT1 in HepG2 cells following transfection. (G) Effects of SIRT6 overexpression on intracellular lipid deposition. PA + lipo group (liposome); PA + pcDNA 3.1 group (liposome + pcDNA 3.1); PA + SIRT6-pcDNA 3.1 group (liposome + SIRT6-pcDNA 3.1). β-actin was used as a control for the normalization of samples for western blotting. Scale bar, 100 μm. Data are presented as the mean ± SD, n=3, $^{\#\#}$P<0.001 vs. PA + pcDNA 3.1 group (one-way ANOVA with Tukey's multiple comparison test). ACC, acetyl-CoA carboxylase; CPT1, carnitine palmitoyl transferase; FASN, fatty acid synthase; NC, negative control; PA, palmitate; PGC1α, PPARγ-coactivator 1α; PPARγ, peroxisome proliferator-activated receptor-γ; SIRT6, sirtuin 6; SREBP1, sterol regulatory element-binding protein 1.

SIRT6 overexpression affects the expression of lipid metabolism-related genes. To further analyze the effect of SIRT6 overexpression on intracellular lipid metabolism, SIRT6-pcDNA 3.1 was transfected into HepG2 cells. The results demonstrated that, after transfection with SIRT6-pcDNA 3.1, the expression levels of SIRT6 mRNA were

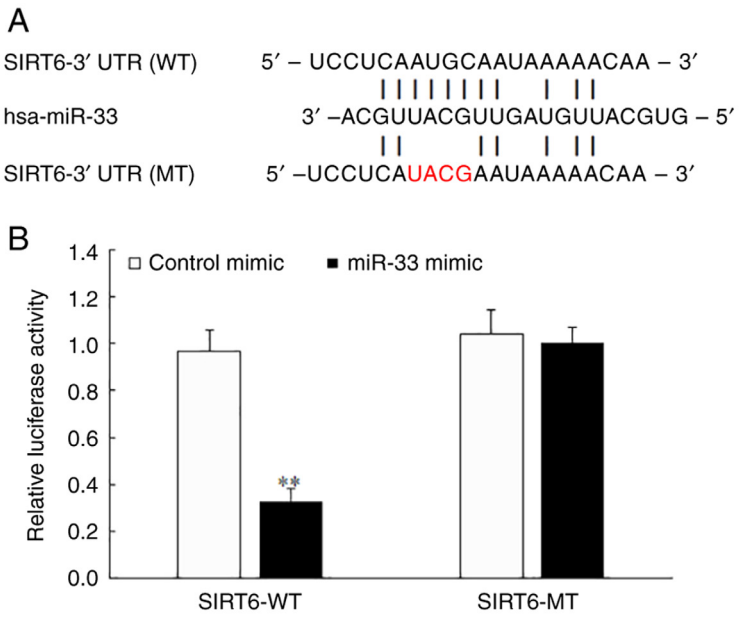

Figure 9. miR-33 binds the 3'-UTR of SIRT6. (A) Target sequence for miR-33 in the SIRT6 3'-UTR. The sequence in red represents mutations of the predicted miR-33 binding site in the SIRT6 3'-UTR. (B) Luciferase reporter assays in 293T cells demonstrating the repressive effect of miR-33 mimics on the activities of the SIRT6 3'-UTR (WT). Data are presented as the mean ± SD (n=3; **P<0.001 vs. control mimics group; unpaired t-test). hsa, *Homo sapiens*; miR, microRNA; UTR, untranslated region; SIRT6, sirtuin 6; WT, wild-type; MT, mutant-type.

significantly increased (Fig. 8A) and the protein expression levels of SIRT6 were also significantly increased compared with those in the pcDNA 3.1 group (Fig. 8B and C). HepG2 cells were induced by PA for 24 h after transfection, and RT-qPCR and western blotting were used to analyze the effect of SIRT6 overexpression on its downstream lipid metabolism-related genes, and Oil Red O staining was used to analyze the effect of SIRT6 overexpression on lipid deposition. The results revealed that transfection of HepG2 cells with SIRT6 overexpression vector increased PPARγ, PGC1α and CPT1 expression, and decreased ACC, FASN and SREBP1 mRNA (Fig. 8D) and protein expression levels (Fig. 8E and F). Simultaneously, Oil Red O staining revealed decreased lipid deposition in HepG2 cells after SIRT6 overexpression (Fig. 8G).

miR-33 binds to the 3'-UTR of SIRT6 mRNA and inhibits SIRT6 expression. To confirm the direct binding of miR-33 to the 3'-UTR of SIRT6 mRNA, luciferase reporter constructs were generated containing the miR-33 binding site (SIRT6-WT) and its mutant sequence (SIRT6-MT). The results of the luciferase reporter assay demonstrated that the miR-33 mimic significantly decreased the luciferase activity in the SIRT6-WT group (Fig. 9A and B) and had no obvious effect in the SIRT6-MT group (Fig. 9B), indicating that SIRT6 was a direct target of miR-33.

Discussion

miRNAs represent a novel level of regulation that could provide novel therapeutic targets for the treatment of numerous human diseases (11,43-47). Manipulating the expression of miRNAs has good potential for treating lipid metabolism (48). miR-33 is one of the most well-studied miRNAs and regulates hepatic lipoprotein metabolism, fibrosis and regeneration (49). Previous studies have reported that short-term treatment with miR-33 inhibitors markedly increased plasma HDL-C levels (50-52). Numerous studies (53-57) have confirmed that Chinese herbal medicines or their active components can target miRNAs in the treatment of diseases. However, few studies (58-60) have focused on the treatment of lipid metabolism disorders with traditional Chinese medicines or their active components targeting miR-33. To this end, in the current study, the *in vivo* and *in vitro* effects of Res were investigated in a HFD mouse model and PA-induced HepG2 cells. The results indicated that Res antagonized abnormal lipid metabolism by targeting miR-33. A further search for downstream genes found that Res inhibited miR-33 expression in the liver and upregulated SIRT6, a key regulator of hepatic lipid metabolism and liver health (61,62). Res also altered the expression levels of genes involved in fatty acid synthesis and fatty acid β-oxidation. Thus, the present study indicated that Res should be further studied for its potential clinical use to prevent or treat hyperlipidemia and associated diseases.

Although multiple animal experiments have confirmed that miR-33 is an important small RNA in regulating lipid metabolism, few studies have been conducted on its expression levels in circulating blood in individuals with hyperlipidemia (20,58,63-67). A total of two studies have confirmed upregulation of miR-33 expression in circulating blood using different methods in participants with hyperlipidemia compared with participants without hyperlipidemia (68,69). Therefore, in the present study, the serum levels of miR-33 were detected in participants with hyperlipidemia. The results showed significant upregulation of miR-33 expression in participants with hyperlipidemia, consistent with previous research findings.

The expression levels of SIRT6, a known target gene of miR-33 (62), were lower in participants with hyperlipidemia

compared with participants without hyperlipidemia. SIRT6 is a member of the class III histone deacetylase family and serves an important role in regulating hepatic TG, TC and LDL-C homeostasis (70-76). SIRT6 also increases hepatic fatty acid oxidation (77). The present findings demonstrated that Res improved the basic metabolic parameters of mice fed a HFD. Res also inhibited miR-33 expression and promoted SIRT6 expression in the HFD mouse models and PA-induced HepG2 cells in the present study. Furthermore, Res treatment altered the expression levels of other genes involved in fatty acid synthesis and fatty acid β-oxidation. Among these genes, SREBP1 can regulate fatty acid homeostasis, and SREBP1 upregulation can lead to lipid metabolism disorders, subsequently causing insulin resistance, obesity, non-alcoholic fatty liver disease and hepatocellular carcinoma (78-81). The activities of both FASN and ACC are an indirect indicator of lipid synthesis in the liver (82). Previous studies have reported that increased activation of FASN and ACC could accelerate lipid synthesis (83,84). In the present study, Res downregulated the protein expression levels of SREBP1, ACC and FASN in the liver of mice fed a HFD. These results indicated that Res decreased lipid synthesis, which prevents excessive accumulation of fat (37). Res also upregulated the protein expression levels of PGC1α, PPARγ and CPT1 in the livers of mice fed a HFD. The aforementioned genes are involved in fatty acid β-oxidation. For example, CPT1 participates in hepatic lipid metabolism and adipocyte differentiation (85,86). CPT1 activation can reduce the number of adipocytes, facilitate adipocyte differentiation and control lipid peroxidation (87). Upregulation of PPARγ in subcutaneous adipose tissue can combat HFD-induced obesity and promote β-oxidation of fatty acids (85,88). PGC1α, as a key PPARγ coactivator, regulates fatty acid catabolism (89). The present results indicated a direct interaction between miR-33 and the SIRT6-3'-UTR. It was also demonstrated that miR-33 negatively regulated SIRT6 protein expression at the post-translational level *in vitro*, and SIRT6 overexpression changed the expression levels of genes involved in fatty acid synthesis and fatty acid β-oxidation. The present results suggested that Res improved lipid metabolism by regulating the miR-33/SIRT6 signaling pathway.

In conclusion, the present study revealed a negative association between miR-33 and SIRT6 expression in hyperlipidemia. miR-33 negatively regulated lipid metabolism by targeting SIRT6. Res improved lipid metabolism by regulating the miR-33/SIRT6 signaling pathway. However, how Res regulated miR-33 expression remains uncertain and requires further investigation in subsequent studies. It is expected that further research can provide additional insights into potential therapeutics for lipid metabolism disorders, such as miR-33 antagonists to reduce the harm caused by elevated blood lipids.

Acknowledgements

Not applicable.

Funding

The present study was supported by the Natural Science Foundation of Hebei (grant no. H201830-7071).

Availability of data and materials

The data generated in the present study may be requested from the corresponding author.

Authors' contributions

CL and GS conceived and designed the study. CL, XP, ZH, XW and CW acquired and analyzed the data. CL, CW and GS confirm the authenticity of all the raw data. CL prepared the draft of the manuscript. All authors read and approved the final manuscript.

Ethics approval and consent to participate

Written informed consent was provided by all participants. Patient studies (2018 Scientific Research Ethics Review; approval no. 39) and animal experiments (2022 Scientific Research Ethics Review; approval no. 217) were approved by the Hebei General Hospital Ethics Committee (Shijiazhuang, China). Animal experiments complied with the Animal (Scientific Procedures) Act 1986 and associated guidelines.

Patient consent for publication

Not applicable.

Competing interests

The authors declare that they have no competing interests.

References

1. Joint Committee on Revision of Guidelines for the Prevention and Treatment of Dyslipidemia in Adults: Guidelines for the prevention and treatment of dyslipidemia in Chinese adults (revised edition 2016). Chin Circul J 31: 937-950, 2016.
2. Mensah GA, Fuster V and Roth GA: A heart-healthy and stroke-free world: Using data to inform global action. J Am Coll Cardiol 82: 2343-2349, 2023.
3. Nelson RH: Hyperlipidemia as a risk factor for cardiovascular disease. Prim Care 40: 195-211, 2013.
4. Klop B, Elte JW and Cabezas MC: Dyslipidemia in obesity: Mechanisms and potential targets. Nutrients 5: 1218-1240, 2013.
5. Chen MY, Meng XF, Han YP, Yan JL, Xiao C and Qian LB: Profile of crosstalk between glucose and lipid metabolic disturbance and diabetic cardiomyopathy: Inflammation and oxidative stress. Front Endocrinol (Lausanne) 13: 983713, 2022.
6. Song R, Hu M, Qin X, Qiu L, Wang P, Zhang X, Liu R and Wang X: The roles of lipid metabolism in the pathogenesis of chronic diseases in the elderly. Nutrients 15: 3433, 2023.
7. Michos ED, McEvoy JW and Blumenthal RS: Lipid management for the prevention of atherosclerotic cardiovascular disease. N Engl J Med 381: 1557-1567, 2019.
8. Agbu P and Carthew RW: MicroRNA-mediated regulation of glucose and lipid metabolism. Nat Rev Mol Cell Biol 22:425-438, 2021
9. Rayner KJ, Suárez Y, Dávalos A, Parathath S, Fitzgerald ML, Tamehiro N, Fisher EA, Moore KJ and Fernández-Hernando C: MiR-33 contributes to the regulation of cholesterol homeostasis. Science 328: 1570-1573, 2010.
10. Marquart TJ, Allen RM, Ory DS and Baldán A: miR-33 links SREBP-2 induction to repression of sterol transporters. Proc Natl Acad Sci USA 107: 12228-12232, 2010.
11. Najafi-Shoushtari SH, Kristo F, Li Y, Shioda T, Cohen DE, Gerszten RE and Näär AM: MicroRNA-33 and the SREBP host genes cooperate to control cholesterol homeostasis. Science 328: 1566-1569, 2010.

12. Price NL, Goedeke L, Suárez Y and Fernández-Hernando C: miR-33 in cardiometabolic diseases: Lessons learned from novel animal models and approaches. EMBO Mol Med 13: e12606, 2021.
13. Deng X, Qin S, Chen Y, Liu H, Yuan E, Deng H and Liu S: B-RCA revealed circulating miR-33a/b associates with serum cholesterol in type 2 diabetes patients at high risk of ASCVD. Diabetes Res Clin Pract 140:191-199, 2018.
14. Price NL, Singh AK, Rotllan N, Goedeke L, Wing A, Canfrán-Duque A, Diaz-Ruiz A, Araldi E, Baldán Á, Camporez JP, *et al*: Genetic ablation of miR-33 increases food intake, enhances adipose tissue expansion, and promotes obesity and insulin resistance. Cell Rep 22: 2133-2145, 2018.
15. Price NL, Rotllan N, Canfrán-Duque A, Zhang X, Pati P, Arias N, Moen J, Mayr M, Ford DA, Baldán Á, *et al*: Genetic dissection of the impact of miR-33a and miR-33b during the progression of atherosclerosis. Cell Rep 21: 1317-1330, 2017.
16. Näär AM: miR-33: A metabolic conundrum. Trends Endocrinol Metab 29: 667-668, 2018.
17. Li T, Francl JM, Boehme S and Chiang JYL: Regulation of cholesterol and bile acid homeostasis by the cholesterol 7α-hydroxylase/steroid response element-binding protein 2/microRNA-33a axis in mice. Hepatology 58: 1111-1121, 2013.
18. Allen RM, Marquart TJ, Albert CJ, Suchy FJ, Wang DQH, Ananthanarayanan M, Ford DA and Baldán A: miR-33 controls the expression of biliary transporters, and mediates statin- and diet-induced hepatotoxicity. EMBO Mol Med 4: 882-895, 2012.
19. Ouimet M, Ediriweera HN, Gundra UM, Sheedy FJ, Ramkhelawon B, Hutchison SB, Rinehold K, van Solingen C, Fullerton MD, Cecchini K, *et al*: MicroRNA-33-dependent regulation of macrophage metabolism directs immune cell polarization in atherosclerosis. J Clin Invest 125: 4334-4348, 2015.
20. Tomita K, Teratani T, Suzuki T, Shimizu M, Sato H, Narimatsu K, Okada Y, Kurihara C, Irie R, Yokoyama H, *et al*: Free cholesterol accumulation in hepatic stellate cells: Mechanism of liver fibrosis aggravation in nonalcoholic steatohepatitis in mice. Hepatology 59: 154-169, 2014.
21. Price NL, Zhang X, Fernández-Tussy P, Singh AK, Burnap SA, Rotllan N, Goedeke L, Sun J, Canfrán-Duque A, Aryal B, *et al*: Loss of hepatic miR-33 improves metabolic homeostasis and liver function without altering body weight or atherosclerosis. Proc Natl Acad Sci USA 118: e2006478118, 2021.
22. Fernández-Tussy P, Sun J, Cardelo MP, Price NL, Goedeke L, Xirouchaki CE, Yang X, Pastor-Rojo O, Bennett AM, Tiganis T, *et al*: Hepatocyte-specific miR-33 deletion attenuates NAFLD-NASH-HCC progression. bioRxiv [Preprint]: 2023.01.18.523503, 2023.
23. Kang J, Kim H, Mun D, Yun N and Joung B: Co-delivery of curcumin and miRNA-144-3p using heart-targeted extracellular vesicles enhances the therapeutic efficacy for myocardial infarction. J Control Release 331: 62-73, 2021.
24. Alharris E, Alghetaa H, Seth R, Chatterjee S, Singh NP, Nagarkatti M and Nagarkatti P: Corrigendum: Resveratrol attenuates allergic asthma and associated inflammation in the lungs through regulation of miRNA-34a that targets FoxP3 in mice. Front Immunol 14: 1130947, 2023.
25. Chen WT, Yang MJ, Tsuei YW, Su TC, Siao AC, Kuo YC, Huang LR, Chen Y, Chen SJ, Chen PC, *et al*: Green tea epigallocatechin gallate inhibits preadipocyte growth via the microRNA-let-7a/HMGA2 signaling pathway. Mol Nutr Food Res 67: e2200336, 2023.
26. Pezzuto JM: Resveratrol: Twenty years of growth, development and controversy. Biomol Ther (Seoul) 27: 1-14, 2019.
27. Huang X and Zhu H: Resveratrol and its analogues: Promising antitumor agents. Anticancer Agents Med Chem 11: 479-490, 2011.
28. Rauf A, Imran M, Suleria HAR, Ahmad B, Peters DG and Mubarak MS: A comprehensive review of the health perspectives of resveratrol. Food Funct 8: 4284-4305, 2017.
29. Zhang W, Yu H, Lin Q, Liu X, Cheng Y and Deng B: Anti-inflammatory effect of resveratrol attenuates the severity of diabetic neuropathy by activating the Nrf2 pathway. Aging (Albany NY) 13: 10659-10671, 2021.
30. Bagul PK, Middela H, Matapally S, Padiya R, Bastia T, Madhusudana K, Reddy BR, Chakravarty S and Banerjee SK: Attenuation of insulin resistance, metabolic syndrome and hepatic oxidative stress by resveratrol in fructose-fed rats. Pharmacol Res 66: 260-268, 2012.
31. Most J, Timmers S, Warnke I, Jocken JW, van Boekschoten M, de Groot P, Bendik I, Schrauwen P, Goossens GH and Blaak EE: Combined epigallocatechin-3-gallate and resveratrol supplementation for 12 wk increases mitochondrial capacity and fat oxidation, but not insulin sensitivity, in obese humans: A randomized controlled trial. Am J Clin Nutr 104: 215-227, 2016.
32. Auger C, Teissedre PL, Gérain P, Lequeux N, Bornet A, Serisier S, Besançon P, Caporiccio B, Cristol JP and Rouanet JM: Dietary wine phenolics catechin, quercetin, and resveratrol efficiently protect hypercholesterolemic hamsters against aortic fatty streak accumulation. J Agric Food Chem 53: 2015-2021, 2005.
33. Fogacci F, Tocci G, Presta V, Fratter A, Borghi C and Cicero AFG: Effect of resveratrol on blood pressure: A systematic review and meta-analysis of randomized, controlled, clinical trials. Crit Rev Food Sci Nutr 59: 1605-1618, 2019.
34. Singh AP, Singh R, Verma SS, Rai V, Kaschula CH, Maiti P and Gupta SC: Health benefits of resveratrol: Evidence from clinical studies. Med Res Rev 39: 1851-1891, 2019.
35. Onuki J, Almeida EA, Medeiros MHG and Di Mascio P: Inhibition of 5-aminolevulinic acid-induced DNA damage by melatonin, N1-acetyl-N2-formyl-5-methoxykynuramine, quercetin or resveratrol. J Pineal Res 38: 107-115, 2005.
36. Fujimoto M, Shimizu N, Kunii K, Martyn JAJ, Ueki K and Kaneki M: A role for iNOS in fasting hyperglycemia and impaired insulin signaling in the liver of obese diabetic mice. Diabetes 54: 1340-1348, 2005.
37. Yarahmadi S, Farahmandian N, Fadaei R, Koushki M, Bahreini E, Karima S, Barzin Tond S, Rezaei A, Nourbakhsh M and Fallah S: Therapeutic potential of resveratrol and atorvastatin following high-fat diet uptake-induced nonalcoholic fatty liver disease by targeting genes involved in cholesterol metabolism and miR33. DNA Cell Biol 42: 82-90, 2023.
38. Baselga-Escudero L, Blade C, Ribas-Latre A, Casanova E, Suárez M, Torres JL, Salvado MJ, Arola L and Arola-Arnal A: Resveratrol and EGCG bind directly and distinctively to miR-33a and miR-122 and modulate divergently their levels in hepatic cells. Nucleic Acids Res 42: 882-892, 2014.
39. Ferdowsian H: Human and animal research guidelines: Aligning ethical constructs with new scientific developments. Bioethics 25: 472-478, 2011.
40. Hickman DL: Minimal exposure times for irreversible euthanasia with carbon dioxide in mice and rats. J Am Assoc Lab Anim Sci 61: 283-286, 2022.
41. American Veterinary Medical Association. [Internet]. 2020. AVMA guidelines for the euthanasia of animals. [Cited 12 January 2022.] Available at: https://www.avma.org/sites/default/files/2020-01/2020-Euthanasia-Final-1-17-20.pdf.
42. Livak KJ and Schmittgen TD: Analysis of relative gene expression data using real-time quantitative PCR and the 2(-Delta Delta C(T)) method. Methods 25: 402-408, 2001.
43. Horie T, Nishino T, Baba O, Kuwabara Y, Nakao T, Nishiga M, Usami S, Izuhara M, Sowa N, Yahagi N, *et al*: MicroRNA-33 regulates sterol regulatory element-binding protein 1 expression in mice. Nat Commun 4: 2883, 2013.
44. Barwari T, Joshi A and Mayr M: MicroRNAs in cardiovascular disease. J Am Coll Cardiol 68: 2577-2584, 2016.
45. Olson EN: MicroRNAs as therapeutic targets and biomarkers of cardiovascular disease. Sci Transl Med 6: 239ps3, 2014.
46. Mahtal N, Lenoir O, Tinel C, Anglicheau D and Tharaux PL: MicroRNAs in kidney injury and disease. Nat Rev Nephrol 18: 643-662, 2022.
47. Wonnacott A, Denby L, Coward RJM, Fraser DJ and Bowen T: MicroRNAs and their delivery in diabetic fibrosis. Adv Drug Deliv Rev 182: 114045, 2022.
48. Ji C and Guo X: The clinical potential of circulating microRNAs in obesity. Nat Rev Endocrinol 15: 731-743, 2019.
49. Gerlach CV and Vaidya VS: MicroRNAs in injury and repair. Arch Toxicol 91: 2781-2797, 2017.
50. Alrob OA, Khatib S and Naser SA: MicroRNAs 33, 122, and 208: A potential novel targets in the treatment of obesity, diabetes, and heart-related diseases. J Physiol Biochem 73: 307-314, 2017.
51. Baselga-Escudero L, Bladé C, Ribas-Latre A, Casanova E, Salvadó MJ, Arola L and Arola-Arnal A: Grape seed proanthocyanidins repress the hepatic lipid regulators miR-33 and miR-122 in rats. Mol Nutr Food Res 56: 1636-1646, 2012.
52. Rayner KJ, Esau CC, Hussain FN, McDaniel AL, Marshall SM, van Gils JM, Ray TD, Sheedy FJ, Goedeke L, Liu X, *et al*: Inhibition of miR-33a/b in non-human primates raises plasma HDL and lowers VLDL triglycerides. Nature 478: 404-407, 2011.

53. Dong Y, Chen H, Gao J, Liu Y, Li J and Wang J: Bioactive ingredients in Chinese Herbal medicines that target non-coding RNAs: Promising new choices for disease treatment. Front Pharmacol 10: 515, 2019.
54. Guo G, Zhou J, Yang X, Feng J, Shao Y, Jia T, Huang Q, Li Y, Zhong Y, Nagarkatti PS and Nagarkatti M: Role of MicroRNAs induced by Chinese Herbal medicines against hepatocellular carcinoma: A brief review. Integr Cancer Ther 17: 1059-1067, 2018.
55. Huang Z, Huang Q, Ji L, Wang Y, Qi X, Liu L, Liu Z and Lu L: Epigenetic regulation of active Chinese herbal components for cancer prevention and treatment: A follow-up review. Pharmacol Res 114: 1-12, 2016.
56. Xin H, Kong Y, Wang Y, Zhou Y, Zhu Y, Li D and Tan W: Lignans extracted from Vitex negundo possess cytotoxic activity by G2/M phase cell cycle arrest and apoptosis induction. Phytomedicine 20: 640-647, 2023.
57. Wu Z, Zhu Q, Yin Y, Kang D, Cao R, Tian Q, Zhang Y, Lu S and Liu P: Traditional Chinese medicine CFF-1 induced cell growth inhibition, autophagy, and apoptosis via inhibiting EGFR-related pathways in prostate cancer. Cancer Med 7: 1546-1559, 2018.
58. Cao R, Bai Y, Sun L, Zheng J, Zu M, Du G and Ye P: Xuezhikang therapy increases miR-33 expression in patients with low HDL-C levels. Dis Markers 2014: 781780, 2014.
59. Su D, Liu H, Qi X, Dong L, Zhang R and Zhang J: Citrus peel flavonoids improve lipid metabolism by inhibiting miR-33 and miR-122 expression in HepG2 cells. Biosci Biotechnol Biochem 83: 1747-1755, 2019.
60. Yang X, Wang L, Zhang Z, Hu J, Liu X, Wen H, Liu M, Zhang X, Dai H, Ni M, *et al*: Ginsenoside Rb_1 enhances plaque stability and inhibits adventitial vasa vasorum via the modulation of miR-33 and PEDF. Front Cardiovasc Med 8: 654670, 2021.
61. Kim HS, Xiao C, Wang RH, Lahusen T, Xu X, Vassilopoulos A, Vazquez-Ortiz G, Jeong WI, Park O, Ki SH, *et al*: Hepatic-specific disruption of SIRT6 in mice results in fatty liver formation due to enhanced glycolysis and triglyceride synthesis. Cell Metab 12: 224-236, 2010.
62. He J, Zhang G, Pang Q, Yu C, Xiong J, Zhu J and Chen F: SIRT6 reduces macrophage foam cell formation by inducing autophagy and cholesterol efflux under ox-LDL condition. FEBS J 284: 1324-1337, 2017.
63. Rayner KJ, Sheedy FJ, Esau CC, Hussain FN, Temel RE, Parathath S, van Gils JM, Rayner AJ, Chang AN, Suarez Y, *et al*: Antagonism of miR-33 in mice promotes reverse cholesterol transport and regression of atherosclerosis. J Clin Invest 121: 2921-2931, 2011.
64. Shao F, Wang X, Yu J, Jiang H, Zhu B and Gu Z: Expression of miR-33 from an SREBF2 intron targets the FTO gene in the chicken. PLoS One 9: e91236, 2014.
65. Zheng Y, Jiang S, Zhang Y, Zhang R and Gong D: Detection of miR-33 expression and the verification of its target genes in the fatty liver of geese. Int J Mol Sci 16: 12737-12752, 2015.
66. D'Onofrio N, Sardu C, Paolisso P, Minicucci F, Gragnano F, Ferraraccio F, Panarese I, Scisciola L, Mauro C, Rizzo MR, *et al*: MicroRNA-33 and SIRT1 influence the coronary thrombus burden in hyperglycemic STEMI patients. J Cell Physiol 235: 1438-1452, 2020.
67. Gnanaguru G, Wagschal A, Oh J, Saez-Torres KL, Li T, Temel RE, Kleinman ME, Näär AM and D'Amore PA: Targeting of miR-33 ameliorates phenotypes linked to age-related macular degeneration. Mol Ther 29: 2281-2293, 2021.
68. Yerlikaya FH, Can U, Alpaydin MS and Aribas A: The relationship between plasma microRNAs and serum trace elements levels in primary hyperlipidemia. Bratisl Lek Listy 120: 344-348, 2019.
69. Simionescu N, Niculescu LS, Sanda GM, Margina D and Sima AV: Analysis of circulating microRNAs that are specifically increased in hyperlipidemic and/or hyperglycemic sera. Mol Biol Rep 41: 5765-5773, 2014.
70. Marmorstein R: Structure and chemistry of the Sir2 family of NAD+-dependent histone/protein deactylases. Biochem Soc Trans 32: 904-909, 2004.
71. Kanfi Y, Peshti V, Gil R, Naiman S, Nahum L, Levin E, Kronfeld-Schor N and Cohen HY: SIRT6 protects against pathological damage caused by diet-induced obesity. Aging Cell 9: 162-173, 2010.
72. Hong J, Mei C, Abbas Raza SH, Khan R, Cheng G and Zan L: SIRT6 cooperates with SIRT5 to regulate bovine preadipocyte differentiation and lipid metabolism via the AMPKα signaling pathway. Arch Biochem Biophys 681: 108260, 2020.
73. Yang Q, Hu J, Yang Y, Chen Z, Feng J, Zhu Z, Wang H, Yang D, Liang W and Ding G: Sirt6 deficiency aggravates angiotensin II-induced cholesterol accumulation and injury in podocytes. Theranostics 10: 7465-7479, 2020.
74. Tao R, Xiong X, DePinho RA, Deng CX and Dong XC: Hepatic SREBP-2 and cholesterol biosynthesis are regulated by FoxO3 and Sirt6. J Lipid Res 54: 2745-2753, 2013.
75. Elhanati S, Kanfi Y, Varvak A, Roichman A, Carmel-Gross I, Barth S, Gibor G and Cohen HY: Multiple regulatory layers of SREBP1/2 by SIRT6. Cell Rep 4: 905-912, 2013.
76. Guo Z, Li P, Ge J and Li H: SIRT6 in aging, metabolism, inflammation and cardiovascular diseases. Aging Dis 13: 1787-1822, 2022.
77. Naiman S, Huynh FK, Gil R, Glick Y, Shahar Y, Touitou N, Nahum L, Avivi MY, Roichman A, Kanfi Y, *et al*: SIRT6 promotes hepatic beta-oxidation via activation of PPARα. Cell Rep 29: 4127-4143.e8, 2019.
78. Ambele MA, Dhanraj P, Giles R and Pepper MS: Adipogenesis: A complex interplay of multiple molecular determinants and pathways. Int J Mol Sci 21: 4283, 2020.
79. Brewer M, Lange D, Baler R and Anzulovich A: SREBP-1 as a transcriptional integrator of circadian and nutritional cues in the liver. J Biol Rhythms 20: 195-205, 2005.
80. Prodanović R, Korićanac G, Vujanac I, Djordjević A, Pantelić M, Romić S, Stanimirović Z and Kirovski D: Obesity-driven prepartal hepatic lipid accumulation in dairy cows is associated with increased CD36 and SREBP-1 expression. Res Vet Sci 107: 16-19, 2016.
81. Feng T, Li S, Zhao G, Li Q, Yuan H, Zhang J, Gu R, Ou D, Guo Y, Kou Q, *et al*: DDX39B facilitates the malignant progression of hepatocellular carcinoma via activation of SREBP1-mediated de novo lipid synthesis. Cell Oncol (Dordr) 46: 1235-1252, 2023.
82. Abukhalil MH, Hussein OE, Bin-Jumah M, Saghir SAM, Germoush MO, Elgebaly HA, Mosa NM, Hamad I, Qarmush MM, Hassanein EM, *et al*: Farnesol attenuates oxidative stress and liver injury and modulates fatty acid synthase and acetyl-CoA carboxylase in high cholesterol-fed rats. Environ Sci Pollut Res Int 27: 30118-30132, 2020.
83. Kastaniotis AJ, Autio KJ, Kerätär JM, Monteuuis G, Mäkelä AM, Nair RR, Pietikäinen LP, Shvetsova A, Chen Z and Hiltunen JK: Mitochondrial fatty acid synthesis, fatty acids and mitochondrial physiology. Biochim Biophys Acta Mol Cell Biol Lipids 1862: 39-48, 2017.
84. Peng X, Li J, Wang M, Qu K and Zhu H: A novel AMPK activator improves hepatic lipid metabolism and leukocyte trafficking in experimental hepatic steatosis. J Pharmacol Sci 140: 153-161, 2019.
85. Mørkholt AS, Oklinski MK, Larsen A, Bockermann R, Issazadeh-Navikas S, Nieland JGK, Kwon TH, Corthals A, Nielsen S and Nieland JDV: Pharmacological inhibition of carnitine palmitoyl transferase 1 inhibits and reverses experimental autoimmune encephalitis in rodents. PLoS One 15: e0234493, 2020.
86. Song S, Attia RR, Connaughton S, Niesen MI, Ness GC, Elam MB, Hori RT, Cook GA and Park EA: Peroxisome proliferator activated receptor alpha (PPARalpha) and PPAR gamma coactivator (PGC-1alpha) induce carnitine palmitoyltransferase IA (CPT-1A) via independent gene elements. Mol Cell Endocrinol 325: 54-63, 2010.
87. Schlaepfer IR and Joshi M: CPT1A-mediated fat oxidation, mechanisms, and therapeutic potential. Endocrinology 161: bqz046, 2020.
88. Sabry MM, Dawood AF, Rashed LA, Sayed SM, Hassan S and Younes SF: Relation between resistin, PPAR-γ, obesity and atherosclerosis in male albino rats. Arch Physiol Biochem 126: 389-398, 2020.
89. Zhang Y, Ma K, Song S, Elam MB, Cook GA and Park EA: Peroxisomal proliferator-activated receptor-gamma coactivator-1 alpha (PGC-1 alpha) enhances the thyroid hormone induction of carnitine palmitoyltransferase I (CPT-I alpha). J Biol Chem 279: 53963-53971, 2004.